Division of Pharmaceutical Technology
Faculty of Pharmacy
University of Helsinki
Finland

Biocompatibility and biofunctionalization of mesoporous silicon particles

Luis Maria Bimbo

ACADEMIC DISSERTATION

To be presented, with the permission of the Faculty of Pharmacy of the University of Helsinki, for public examination in Auditorium 1041 at Biocenter 2, (Viikinkaari 5 E), on February 4th, 2012, at 12.00 noon.

Helsinki 2012

Supervisors   Docent Hélder Almeida Santos
Division of Pharmaceutical Technology
Faculty of Pharmacy
University of Helsinki
Finland

Professor Jouni Hirvonen
Division of Pharmaceutical Technology
Faculty of Pharmacy
University of Helsinki
Finland

Reviewers   Professor Clive A. Prestidge
The ARC Special Research Centre for Particle and Material
Ian Wark Research Institute
University of South Australia
Australia

Professor Patrick Augustijns
Laboratory for Pharmacotechnology and Biopharmacy
Faculty of Pharmaceutical Sciences
Catholic University of Leuven
Belgium

Opponent   Professor Mauro Ferrari
Department of Nanomedicine
The Methodist Hospital Research Institute
United States of America

Abstract

Several of the newly developed drug molecules experience poor biopharmaceutical behavior, which hinders their effective delivery at the proper site of action. Several strategies are currently being employed in order to overcome this obstacle, namely by associating the drug molecules with suitable carriers. Mesoporous silicon-based materials have emerged as promising drug carriers due to their ability to improve the dissolution behavior of several poorly water-soluble drugs compounds confined within their pores. The aim of this thesis was to investigate the biocompatibility, cellular interaction, drug release and biodistribution of different types of surface treated porous silicon (PSi) micro- and nanoparticles, such as thermally oxidized (TOPSi) and thermally hydrocarbonized (THCPSi).

Studies conducted on TOPSi and THCPSi particles have showed that nanoparticles have a higher degree of biocompatibility than microparticles in RAW 264.7 macrophages and Caco-2 cells. The TOPSi and THCPSi nanoparticles improved the permeability of Caco-2 cell monolayers for the drug compounds indomethacin and griseofulvin. However, both types of surface treated particles were found not to permeate across the differentiated Caco-2 cell monolayers even after 24 h incubations, but were readily internalized by RAW 264.7 macrophages. In addition, the degradation of the nanoparticles showed its potential to fast clearance in the body. Radiolabeled nanoparticles administered intravenously in rats were found to be quickly translocated to liver and spleen, without apparent toxic effects. These results constituted the first quantitative analysis of the behavior of orally administered THCPSi nanoparticles compared with other delivery routes in rats.

The self-assemble of a hydrophobin class II (HFBII) protein at the surface of THCPSi particles endowed the particles with greater biocompatibility in different cell lines (AGS, Caco-2 and HT-29) and was also found to reverse their hydrophobicity and protected a drug loaded within its pores against premature release at low pH (1.2), while enabling subsequent drug release as the pH was increased. The permeability of the drug compound across a differentiated Caco-2 monolayer was undisturbed by the presence of the HFBII-coating and was found to be higher for the coated and uncoated THCPSi particles than for the bulk drug. The protein-coated particles were also found to increase cell association *in vitro* and to promote gastroretentivity *in* vivo. These results highlight the potential of HFBII-coating for PSi-based drug carriers in improving their hydrophilicity, biocompatibility and pH responsiveness in drug delivery applications.

In conclusion, mesoporous silicon particles have been shown to be a versatile platform for improving the dissolution behavior of poorly water-soluble drugs with high biocompatibility and easy surface modification. The results of this study also provide information regarding the biofunctionalization of the THCPSi particles with a fungal protein, leading to an improvement in their biocompatibility and endowing them with pH responsive and mucoadhesive properties.

Acknowledgements

I would like to express my deepest gratitude to my supervisor, Professor Jouni Hirvonen, for his trust, support, guidance, and encouragement. His positive attitude towards life and science has made me realize how lucky I have been to pursue my endeavor in Finland.

I am also extremely grateful to my supervisor Docent Hélder Almeida Santos for all his trust, his unwavering support, belief in my abilities when I found myself doubting them, his ever enthusiastic attitude towards science and his friendship which I greatly cherish and hope to be everlasting.

To all my co-authors, for their invaluable scientific input and fruitful discussions, I would like to extend my deepest gratitude. I would also like to single out Docent Jarno Salonen, Ermei Mäkilä, Docent Timo Laaksonen, Mirkka Sarparanta and Docent Anu J. Airaksinen for all their permanent collaboration and productive discussions.

I would like to express my sincere gratitude to Professor Clive Prestidge and Professor Patrick Augustijns for their review of this thesis and for their constructive comments for its improvement.

I am also extremely grateful to all my colleagues at the Division of Pharmaceutical Technology for the pleasant working atmosphere and for letting me share a part of their lives with me. It is remarkable how such unique camaraderie can thrive in the competitive environment of the academia.

To my Fellow Swordsmen at the Helsinki branch of Kashima Shinryū Ari, Peter, Jari, Vesa, Heikki, Miika and Ilari, I would like to thank for welcoming me with open arms and steadfast patience with such a poor student. Your attitude towards life and learning has inspired and motivated me, and made my stay in Finland even more pleasant.

To Vânia, for her encouragement and love during all this time, I would like to express my most sincere gratitude. I hope we can enjoy more pleasant moments together.

I would also like to thank my brothers Nuno and João, which have also embarked with me on this journey in pursuit of knowledge and share all the joys and frustrations of a scientific career. I have in them my most fierce critics and one of my greatest sources of inspiration and improvement.

Finally, I would like express my everlasting gratitude and dedicate this dissertation to my father Luís and mother Isabel, for all their unwavering support, their love and encouragement, for their unflinching belief in me, and for always inspiring me to learn more. I have been truly blessed for sharing my life with you.

Contents

List of original publications

This thesis is based on the following original publications, which are referred in the text by their roman numerals I-V:

I   **Bimbo L.M.**, Mäkilä E., Laaksonen T., Lehto V.-P., Salonen J., Hirvonen J., Santos H.A., 2011. Drug permeation across intestinal epithelial cells using porous silicon nanoparticles. *Biomaterials* 32(10):2625−2633.

II   **Bimbo L.M.**, Sarparanta M., Santos H.A., Airaksinen A.J., Mäkilä E., Laaksonen T., Peltonen L., Lehto V.-P., Hirvonen J., Salonen J., 2010. Biocompatibility of thermally hydrocarbonized porous silicon nanoparticles and their biodistribution in rats. *ACS Nano* 4(6):3023−3032.

III   **Bimbo L.M.**, Mäkilä E., Raula J., Laaksonen T., Laaksonen P., Strommer K., Kauppinen E.I., Salonen J., Linder M.B., Hirvonen J., Santos H.A., 2011. Functional hydrophobin-coating of thermally hydrocarbonized porous silicon microparticles. *Biomaterials* 32(34): 9089−9099.

IV   **Bimbo L.M.**, Sarparanta M., Mäkilä E., Laaksonen T., Laaksonen P., Salonen J., Linder M.B., Airaksinen A.J., Hirvonen J., Santos H.A., 2011. Cellular interactions and drug permeation of hydrophobin-coated porous silicon nanoparticles. *Nanomedicine – Nanotechnology, Biology and Medicine* (Submitted).

V   Sarparanta M., **Bimbo L.M.**, Mäkilä E., Salonen J., Laaksonen P., Kerttuli H., Linder M.B., Hirvonen J., Laaksonen T., Santos H.A., Airaksinen A.J., 2011. The Mucoadhesive and Gastroretentive Properties of Hydrophobin-Coated Porous Silicon Nanoparticle Oral Drug Delivery Systems. *Biomaterials* (Accepted).

The original publications were reprinted with permissions from the publishers. In publications **II** and **V** the first two authors had equal contributions to the work. In these publications Mirkka Sarparanta designed and carried out the radiolabelling and *in vivo* evaluation of the nanoparticles and the results will be included in her thesis.

Abbreviations

AP-1	Activator protein 1
APTES	3-aminopropyltriethoxysilane
BCA	Bicinchoninic acid
BET	Brunauer-Emmett-Teller
BJH	Barrett-Joyner-Hallenda
BSA	Bovine serum albumin
Da	Dalton
DCM	Dichloromethane
DMEM	Dulbecco's Modified Eagle Medium
DMF	Dimethylformamide
DMSO	Dimethyl sulfoxide
DSC	Differential scanning calorimetry
e.g.	*exempli gratia*
EtOH	Ethanol
FaSSIF	Fasted state simulated intestinal fluid
FDA	Food and Drug Administration
FITC	Fluorescein isothiocyanate
FTIR	Fourier transform infrared spectrsocopy
GI	Gastrointestinal
GSH	Glutathione
GSSG	Glutathione dissulfide
HBSS	Hank's Balanced Salt Solution
HEPES	4-(2-hydroxyethyl)-1-piperazineethanesulfonic acid
HF	Hydrofluoric acid
HFB	Hydrophobin
HFBII	Hydrophobin class II
HNO_3	Nitric acid
HPLC	High perfomance liquid chromatography
i.v.	intravenous
IMC	Indomethacin
IUPAC	International Union of Pure and Applied Chemistry
LDH	Lactate dehydrogenase
LPSiNPs	Luminescent porous silicon nanoparticles
MAP	Mitogen activated protein
MES	2-(*N*-morpholino)ethanesulfonic acid
Mg	Magnesium
NF-κB	Nuclear factor kappa B
NO	Nitric oxide
Nrf2	Nuclear factor (erythroid-derived 2)-like 2
PBS	Phosphate buffer solution
PCL	Polycaprolactone
PEG	Poly(ethylene) glycol

PSi	Porous silicon
PT pore	Permeability transition pore
Pt	Platinum
RES	Reticuloendothelial system
ROS	Reactive oxygen species
RPMI	Roswell Park Memorial Institute
S1MPs	Stage 1 microparticles
S2NPs	Stage 2 nanoparticles
SEM	Scanning electron microscope
SHPP	N-succinimidyl-3-(hydroxyphenyl) propionate
Si	Silicon
$Si(OH)_4$	Silicic acid
SiO_2	Silicon dioxide
TCPSi	Thermally carbonized porous silicon
TEER	Transepithelial electrical resistance
TEM	Transmission electron microscope
THCPSi	Thermally hydrocarbonized porous silicon
TLC	Thin layer chromatography
TOPSi	Thermally oxidized porous silicon

1 Introduction

The recognition that unfavorable physicochemical properties of many drug compounds affect their bioavailability and consequently the efficacy of the treatment, has led to intense research in the field of drug delivery. It has been reported that nearly 50% of all the newly developed lead optimization compounds entering the development pipeline fail because of non-optimal physicochemical and biopharmaceutical properties (Singh *et al.*, 2011). A substantial factor that prevents the development of such substances is the limited dissolution rate. There are currently several strategies employed in order to increase the dissolution behavior of poorly water-soluble drugs, such as oral lipid-based (Hauss, 2007), amorphous formulations (Kawakami, 2009), or delivery systems, such as cyclodextrins (Loftsson *et al.*, 2007; Loftsson and Brewster, 2010).

In order to overcome some of the barriers of drug absorption in the body, the study of drug delivery systems has been actively pursued in the last decades (Hoffman, 2008). The idea of a drug carrier, which would deliver the drug compounds at the appropriate site of action and at the same time maintaining the physiological milieu undisturbed has been long sought after and holds tremendous economical potential. The drug delivery market is one of the most profitable areas within the pharmaceutical industry with about $94 billion value and a 10% annual increase worldwide in 2010 (GBI-Research, 2010). However, the material properties of drug carriers very often also affect the drug's fate, drug release rate, toxicity of the drug carriers, as well as the drug carrier's biocompatibility and safety (Karp and Langer, 2007; Kohane and Langer, 2010).

In addition to the safety and biocompatibility, drug delivery systems should also encompass high payloads, protect the drug against degradation, allow the release of an effective drug concentration at the appropriate site of action and allow some degree of control over the drug's pharmacokinetic distribution profile (Peer *et al.*, 2007). Therefore, the materials used in biomedical applications should be suitably designed in order to achieve a specific biological response, which can derive from the control exerted over their mechanical properties, surface microstructure, texture, porosity and compartmentalization (Mitragotri and Lahann, 2009).

Along with the material properties of the carriers, their physical dimensions and shape were also found to greatly impact their drug delivering properties. Materials at nanoscale have been found to encompass very advantageous mechanical, electrical, chemical and optical features, which are currently being exploited for numerous applications (West and Halas, 2003; Chopra *et al.*, 2007). In the material sciences field, nanomaterials are engineered structures with at least one dimension bellow 100 nanometers (nm) (Nel *et al.*, 2006), although in the pharmaceutical science field this definition has been used rather loosely and might include structures up to 1 µm in either dimension. By taking advantage of the valuable properties of nanoscale delivery systems, such as increased surface area, improved solubility of hydrophobic drugs, possibility to encapsulate and protect drugs from degradation and reduced immunogenic potential and toxicological effect, further developments and innovative drug delivery systems can still be engineered (Couvreur and Vauthier, 2006).

However, these nano-sized drug delivery systems can also elicit undesired biological or toxicological effects (Oberdorster, 2010). This can be related to their own size, shape and surface chemistry (Jiang *et al.*, 2008; Mitragotri and Lahann, 2009; Yoo *et al.*, 2010; Yoo *et al.*, 2011), as well as other hazards resulting from the fabrication process. Nano-engineered structures have been shown to display different stability, behavior in the biological microenvironment, and cellular distribution according to their dimensions, morphology and chemical constitution. Safety and biocompatibility of these engineered structures is, therefore, a requirement both in manufacture and, more importantly, when *in vivo* exposure or administration is concerned. Therefore, in order for a drug delivery carrier to be deemed suitable, it should prove its efficacy along with its safety when administered in the body.

Mesoporous materials, are materials containing pores with diameters between 2 and 50 nm (Rouquerol *et al.*, 1994) and meet some of the aforementioned requirements for drug delivery systems. Their large surface area (> 700 m^2/g) and large pore volume (> 0.9 cm^3/g) can enable their use as drug reservoirs for storing hydrophobic molecules, while allowing an easy tailoring of the pore size (Santos *et al.*, 2011). The drug loading properties and cellular interaction of mesoporous materials can be further modulated by tuning their shape, size, pore or surface functionalization. In addition, mesoporous materials have a well-defined structure and surface, are relatively inexpensive, thermally stable and chemically inert (Salonen *et al.*, 2008).

Among several mesoporous materials that can be found in the literature, porous silicon (PSi) has attracted significant attention due to its interesting properties that enable it to be employed in several biomedical applications (He *et al.*, 2010), such as drug delivery carriers or implantable devices (Zangooie *et al.*, 1998; Canham *et al.*, 1999; Desai *et al.*, 1999; Stewart and Buriak, 2000; Anglin *et al.*, 2008; Salonen *et al.*, 2008). In addition to its drug delivery properties, PSi was also found to be biocompatible (Canham, 1995) and biodegradable (Park *et al.*, 2009). The biodegradation of PSi can even be modulated to some extent by controlling overall porosity, pore size, shape, surface and bulk properties (Canham, 1997). The drug loading degree of PSi was also shown to be affected by several properties of the material, such as hydrophilicity/hydrophobicity, pore size, surface chemistry, loaded compound (charge, chemical nature, shape and molecular size), and drug loading method (Salonen *et al.*, 2005; Limnell *et al.*, 2007; Prestidge *et al.*, 2008). The fabrication method even allows the PSi to remain stable under the stringent conditions of the stomach and gastrointestinal (GI) lumen, while maintaining its advantageous drug delivering properties (Salonen *et al.*, 2008). The challenges of engineering PSi carriers, which can successfully deliver their drug payloads at the site of action while maintaining a tolerable toxic profile, are still partially unmet. A thorough understanding of the biological phenomena surrounding the interaction of PSi materials with the physiological environment, *in* vitro/*vivo*, is therefore, required in order for this material to fulfill its promise as a suitable drug delivery system.

The objectives of this dissertation were to thoroughly characterize PSi particles of different sizes and surface chemistries by several well-established analytical techniques and to assess the biocompatibility and biodistribution of plain and protein-coated PSi particles, along with the corroboration of its potential to increase drug dissolution. For that purpose the following approaches were conducted: (1) visual characterization employing several

microscopy techniques; (2) assessment of cellular viability, reactive oxygen species (ROS) and inflammatory response; (3) loading with poor water-soluble drugs and assess their dissolution and permeation behaviour; (4) evaluation of biocompatibility and cellular association of the protein-coated particles; and finally (5) biodistribution studies in rats.

2 Review of the literature

2.1 Solubility of drug compounds

The goal of pharmacological therapy is to elicit a response from drug administration which can reverse a pathological condition (Chan and Holford, 2001). Such response is dependent on the availability of the active drug at the receptor site, which in turn is influenced by the plasma drug concentrations (Smolen, 1978). The water solubility of a compound is therefore a crucial parameter for the drug to be effective at the target site. By definition, and according to the International Union of Pure and Applied Chemistry (IUPAC), "the analytical composition of a saturated solution, expressed in terms of the proportion of a designated solute in a designated solvent, is the solubility of that solute". The solubility may be expressed as a concentration, molality, mole fraction, mole ratio, etc. (McNaught and Wilkinson, 1997). Chemical entities can be therefore divided according to their solubility, into highly or poorly soluble. In the U.S. and Eur. Pharmacopoeias, the solubility is stated by the descriptive terms shown in Table 1.

Table 1   *Descriptive terms for the solubility used in the pharmacopoeias (USP, 2009; Ph. Eur., 2009).*

Term	Parts of solvent required for 1 part of solute
Very soluble	Less than 1
Freely soluble	From 1 to 10
Soluble	From 10 to 30
Sparingly soluble	From 30 to 100
Slightly soluble	From 100 to 1000
Very slightly soluble	From 1000 to 10 000
Practically insoluble, or insoluble	Greater than or equal to 10 000

Furthermore, in order for a compound to be effectively absorbed in the body, orally-administered drugs need also to be dissolved at the site of absorption in the GI tract (Avdeef, 2001). Then, the compounds are required to transverse several lipid barriers in order to find their way into the systemic circulation. The ability of a compound to diffuse across lipid membranes is termed permeation and is directly correlated with the drug's lipophilicity. It is therefore required that besides possessing some degree of aqueous solubility, the drug displays adequate permeability. Highly-permeable drugs are generally those with an extent of absorption greater than or equal to 90% and are not generally associated with any documented instability in the GI tract (Martinez and Amidon, 2002). However, even if the drug has reasonable membrane permeation properties, the rate-limiting process of absorption is still the drug dissolution step (Singh *et al.*, 2011).

The pharmaceutical research of new chemical entities has reached a stage where poorly water-soluble drug compounds (< 1 μg/ml) are a considerable bottleneck in the drug discovery pipeline (Lipinski *et al.*, 1997; Lipinski, 2000). In order to overcome this difficulty and even to reinstate the research of molecules that exhibited adequate efficacy, but were excluded by their unfavorable physicochemical properties, several strategies can be employed. One strategy to improve the drug's bioavailability, as well as its pharmacological and therapeutic properties with reduced collateral effects, is to associate

the compounds with another entity which serves as a carrier agent. This approach for the delivery of drug compounds can be termed carrier-mediated drug delivery, which allows poorly water-soluble drugs to be confined within the carrier. In this case, the drug can be delivered at the site of absorption and also targeted to a specific site while being sheltered from any unwarranted degradation (Singh *et al.*, 2011). A carrier or drug delivery agent can be basically described as a formulation that controls the rate and period of drug delivery and can target specific areas of the body (Poznansky and Juliano, 1984).

Mesoporous materials, *i.e.* materials which have pores with dimensions between 2 and 50 nm, have been found to be excellent candidates for drug delivery systems due to their unique features, such as a high pore volume, capable of hosting the required amount of compounds; high surface area, which implies high potential for drug adsorption; and tunable pore size with a narrow distribution, which enables a reproducible loading and release of the compounds (Vallet-Regí *et al.*, 2007). When the drug molecules are loaded in the microfabricated porous materials, many of the abovementioned dissolution-related problems can be overcome. The crystalline drug is restricted by the confined space of the pores (usually not much larger than the drug molecule), retaining the drug in its amorphous (non-crystalline) disordered form (Salonen *et al.*, 2005). Consequently, an increase in solubility and dissolution rate of the drugs is achieved as a result of the low lattice energy (high Gibbs free energy) of the amorphous state. The confinement of the compounds within the pores of mesoporous materials allows the attainment of high local drug concentrations and even drug supersaturation, thus increasing the net absorption and respective permeation across biological barriers (Kaukonen *et al.*, 2007; Brouwers *et al.*, 2009). One of the structures that has shown great promise in the confining and release of poorly water-soluble drug compounds was PSi which has been also actively investigated for biomedical applications (Salonen *et al.*, 2008).

2.2 Porous silicon (PSi)

Although silicon (Si) does not occur in nature in free form, in its combined form it accounts for nearly 25% of the earth's crust (Yaroshevsky, 2006). Si-based compounds are distinctive materials both in terms of their chemistry and in their numerous useful applications. Si in combination with organic compounds provides unique properties that function over a wide range of temperature, making these products less temperature sensitive than most organic surfactants. These properties can be credited to the strength and flexibility of the Si-O bond, its partial ionic character and the low interactive forces between the non-polar methyl groups, characteristics that are directly related to the comparatively long Si-O and Si-C bonds. The length of the Si-O and Si-C bonds also allows an unusual freedom of rotation, which enables the molecules to adopt the lowest energy configuration at interfaces, providing a surface tension that is substantially lower than that of organic polymers (O'Lenick, 2009).

One interesting form of Si is PSi, which incorporates varying porosity in its structure, rendering a large surface-to-volume ratio of above 500 m^2/cm^3. The discovery of PSi was made accidentally by Arthur Uhlir Jr. and Ingeborg Uhlir in 1956 at Bell Labs (Uhlir, 1956). Their initial purpose was to develop a technique for polishing and shaping the surfaces of Si and germanium. However, they found that under several conditions, a rough

product in the form of a thick black, red or brown film was formed on the surface of the material. At the time, these findings were only referred as a scientific oddity and briefly mentioned in their technical notes, without noting their porous structure. It was Watanabe and co-workers who first reported their porous nature (Watanabe and Sakai, 1971), but it was not until the late 1980s that Leigh Canham and simultaneously Lehmann and Gösele speculated that the diaphanous Si filaments generated when the pores became large and numerous enough to interconnect, might exhibit quantum confinement effects (Canham, 1990; Lehmann and Gosele, 1991). In addition, it was discovered that the Si wafers could emit visible light at room temperature if subjected to electrochemical and chemical dissolution. These findings led to a substantial amount of research focused on the development of Si-based optoelectronic switches, displays and lasers (Soref, 1993; Canham *et al.*, 1996). However, due to the material's mechanical and chemical instability and its low electroluminescence efficiency, most of the interest in that field subsequently faded. Nonetheless, due to its other remarkable characteristics, such as large surface area-to-volume ratio, the ability to fine tune its pore size, its surface chemistry and the established microfabrication technologies, PSi application were further investigated in several other fields such as Si membranes (Chu *et al.*, 1999) and drug delivery carriers (Anglin *et al.*, 2008; Salonen *et al.*, 2008; Serda *et al.*, 2011).

2.2.1 Manufacture and properties

There have been several methods reported in the literature for the fabrication of PSi materials. The most frequent method is electrochemical anodization of monocrystalline silicon wafers in aqueous ethanolic hydrofluoric acid (HF) electrolytes (Salonen and Lehto, 2008). In its simpler setup, the Si wafer acts as anode while a platinum (Pt) plate serves as a cathode, when both are immersed in the HF-ethanolic solution and current is applied (Figure 1). The almost exclusive use of Pt as a cathode material is due to the fact that Pt is practically the only conductive material which can repeatedly withstand the stringent cathodic conditions. The cell in which the anodization takes place must also be made of HF-resistant material in order to endure the whole etching process. The core properties of the obtained PSi, such as porosity, pore layer thickness, pore size and shape are all determined by the fabrication conditions (Salonen *et al.*, 2000). These conditions include current density, wafer type and resistivity, HF concentration, chemical composition of the electrolytes, crystallographic orientation, temperature, time, electrolyte stirring, illumination intensity and wavelength. All these conditions are very difficult to control completely during the fabrication process. However, as the majority of these parameters are somehow related to each other and can be kept constant, a satisfactory degree of reproducibility can be achieved.
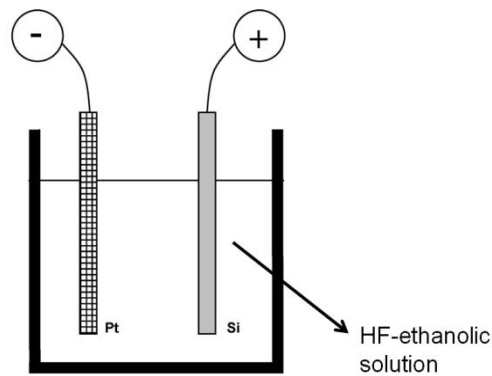
Figure 1 *Schematic representation of a simple etching setup for PSi fabrication. Pt is the cathode and the Si wafer the anode in a HF-ethanolic solution. Modified from Salonen and Lehto, 2008. Copyright © (2008) Elsevier. Reprinted with permission.*

The doping levels of the initial Si wafer were also found to influence the pore morphology of the PSi (Zhang, 2001). Based on the doping levels of the substrate, the Si wafers can be divided into n, n+, p and p+-type, where n- and n+-type Si is usually doped with antimony or phosphorous and p- and p+-type Si with boron. With p type, the pore size increases with dopant concentration, whereas with n-type, the low dopant concentration generates usually macropores, while increasing to higher dopant levels causes mesopores to form (Lehmann *et al.*, 2000). The n-type Si usually yields pores with larger diameters than the p-type, and the pores seem to form straighter cylindrical structures in the <100> direction (Levy-Clement, 1995).

The HF concentration in the electrolyte can also modulate the pore morphology. By decreasing the HF concentration, the pore diameter increases in the Si substrate (Halimaoui, 1997; Zhang, 2001) and pores become straighter and smoother. The use of electrolyte diluting agents other than water (*e.g.* ethanol) has also been found to lead to the formation of smoother and larger pores. The pore shapes are frequently observed to be cylindrical (or spherical), but rectangular pores have also been reported, at least in n-type PSi (Smith and Collins, 1992; Cullis *et al.*, 1997).

Despite the fact that electrochemical anodization is the method most commonly used to fabricate PSi, the stain etching method can also be employed. This method resembles the electrochemical etching, but is based completely on chemical reactions, without the use of any additional current (Archer, 1960; Fathauer *et al.*, 1992; Shih *et al.*, 1992; Kolasinski, 2005). In stain etching, the hole generation is also required, but for this purpose an oxidant is added in the HF electrolyte, usually HNO_3 (Liu *et al.*, 1994; Parbukov *et al.*, 2001; Guerrero-Lemus *et al.*, 2003). The rate of PSi layer growth is directly proportional to the concentration of HNO_3, irrespective of the substrate resistivity. In aqueous HF and HNO_3 solutions, the cathodic reactions produce NO, because it serves as the hole-injector, enabling the Si dissolution. One disadvantage of stain etching is the heterogeneous etching profile, due to the fact that both the cathodic and anodic sites are randomly, but constantly,

present on the Si surface during etching. The other disadvantage of stain etching is the limited thickness of the PSi layer formed, and also the poorer reproducibility compared with the PSi samples produced by anodization. However, recent reports concerning the stain etching method have shown promising results regarding a more controlled and thicker stain etched PSi layers using non-conventional etching solutions (Kolasinski *et al.*, 2010). Another method of PSi fabrication is by photosynthesis, where visible-light irradiation alongside a HF electrolyte was used to produce PSi without the need of any electrodes for anodization (Noguchi and Suemune, 1993). A method relying on ball milling combined with pressing sintering procedures has also been described in the literature for the fabrication of PSi (Jakubowicz *et al.*, 2007). In addition, a method relying on solid flame synthesis, where PSi is formed as Si dioxide (SiO_2) reacts with Mg in a combustion chamber followed by an acid treatment, has also been reported (Won *et al.*, 2009).

2.2.2 Surface chemistry and stabilization

Following anodization, the PSi surface is hydrogen terminated ($Si-H_x$). These bonds can be hybrids Si-H, $Si-H_2$ and $Si-H_3$ and render the Si surface prone to oxidation even in dry ambient air (Burrows *et al.*, 1988; Canham *et al.*, 1991; Salonen *et al.*, 2008; Salonen and Lehto, 2008). Already in the 1960s, Beckmann found out that PSi films were clearly aged when they were stored at ambient air for an extended period (Beckmann, 1965). This was due not only to the native oxidation of PSi, but also due to some other reactions resulting from the storage conditions (Loni *et al.*, 1997). The rate and extent of oxidation from the hydrophobic hydrogen termination to hydrophilic oxidized surface takes a few months at room temperature. Complete native oxidation takes much longer time, depending on the storage conditions. In addition, there are also some impurities present in the PSi, which are commonly detected after the fabrication procedure, such as fluorine, oxygen and trace amounts of hydrocarbons (Grosman and Ortega, 1997). For most applications, a non-reactive and stable surface is crucial, and the unstable hydrogen termination of the freshly etched PSi has to be replaced. By converting the reactive groups into a more stable oxidized, hydrosilylated or (hydro) carbonized form, the PSi surface can be modified even further in terms of hydrophilicity and resistance to oxidation (Table 2).

Table 2 *Surface chemistries, typical Si bonding, hydrophilicity and resistance to oxidation of as-anodized and several surface-treated PSi.*

Surface chemistry	Bonds	Hydrophilicity	Resistance to oxidation
As-anodized	Si-H	-	-
Thermally oxidized	Si-O	++	+
Thermally carbonized	Si-C	+	++
Thermally hydrocarbonized	Si-C-H	-	+++

2.2.2.1 Thermal oxidation

The stabilization of the anodized Si surfaces by thermal oxidation is one of the more straightforward ways to oxidize Si surfaces; the product of this treatment is called thermally oxidized PSi (TOPSi) (Petrova-Koch *et al.*, 1992; Salonen *et al.*, 1997). The

modification of the PSi surface chemistry via thermal oxidation has been extensively studied and has demonstrated the conversion of the native Si_ySiH_x surface to O_ySiH, O_ySiOH and $SiOSi$ (Kumar *et al.*, 1993; Takazawa *et al.*, 1994; Mawhinney *et al.*, 1997). The thermal oxidation starts to occur at a threshold temperature near 250 ºC where there is the first evidence for loss of hydrogen from the Si surface, and where the Si dangling bond sites produced are able to chemisorb O_2 dissociatively, leading to the first stage of surface oxidation. Oxidation leads to O insertion into Si-Si back-bonds, producing $-O_ySiH_x$ species. Oxidation also leads to the formation of surface Si-OH species as a result of the O insertion into Si-H bonds. The subsequent formation of Si-O-Si modes is originated from oxidation of the PSi surfaces (Mawhinney *et al.*, 1997). This method, depending on the treatment temperature, forms a thin layer of SiO_2 on the surface of PSi, resulting in a slight decrease in pore diameter. In addition, the oxidation changes the surface from hydrophobic to hydrophilic (Salonen *et al.*, 2008). Besides thermal oxidation, anodic, photo and chemical oxidation can also be employed on the Si surface (Canham, 1990; Li *et al.*, 1993; Halimaoui, 1997). The fact that the thermal oxidation changes the silicon surface from hydrophobic to hydrophilic renders the material more compatible with the body´s aqueous environment, which is crucial in order to minimize inflammation and enhance biocompatibility (Hezi-Yamit *et al.*, 2009).

2.2.2.2 Thermal hydrocarbonization

It is also possible to obtain a hydrocarbon terminated surface using thermal decomposition of acetylene. This method allows the surface treatment to be conducted at a lower temperature, since there is a threshold temperature which changes the thermal functionalization of PSi into carbonization. The threshold temperature, however, allows a continuous flow of acetylene to be used without any graphitization problems. At treatment temperatures below 700 °C, the hydrogen atoms remain on the PSi surface making it hydrophobic (Si-C-H bonds; thermally hydrocarbonized PSi, THCPSi). (Salonen *et al.*, 2004). The thermal carbonization with acetylene changes surface structure, whereas the silylation reactions change the the surface Si-H chemistry. The use of the small gaseous molecule acetylene in the process has some advantages, such as faster and better diffusion in the pores, which improves the efficiency of surface coverage. This surface treatment has some important advantages compared with the carbonized surface, *e.g.* it is still hydrophobic; the treated layer is thin; and the gas adsorption properties are different from those found in the thermal carbonized (TC) PSi surface (Salonen *et al.*, 2004). Functionalization of THCPSi by radical coupling of sebacic acid has been also reported, as well as their capability to further modify the surface using standard bioconjugate chemistry methods (Sciacca *et al.*, 2010). The authors stated that the material was obtained at 500 °C, thus confirming the THC surface. The surface was stable and comparable to a non-functional thermal oxide, but superior to the widely used carboxyl-terminated surface prepared by the thermal hydrosilylation route.

2.2.2.3 Other surface treatments

Besides the aforementioned treatments to the PSi surfaces, which modulate the surface in terms of its hydrophilicity and resistance to oxidation, other treatments which allow further functionalization of the Si surface have also been reported. The thermal carbonization was one of the first methods employed to stabilize the silicon surface, involving chemical derivations of the PSi surface with organic compounds and formation of Si-C bonds (Dubin *et al.*, 1995; Linford *et al.*, 1995; Sailor and Song, 1998). When the temperature is above 700 °C the formed surface is hydrogen free and more hydrophilic than the material produced at lower temperatures Early works in this area focused on single-crystal reactions that involved heating, which in turn can potentially damage the fragile nanoscale architecture of the PSi, and the use of likely contaminating late transition metals or high vacuum conditions (Buriak, 1999). Subsequently, several groups have also investigated the formation of Si-C bonds on porous silicon at room temperature using one- or two-step wet chemical techniques (Buriak and Allen, 1998; Buriak and Stewart, 1998; Kim and Laibinis, 1998). Stability studies of differently stabilized PSi samples have shown that the TCPSi is an even more efficient stabilizing method than the thermal oxidation (Björkqvist *et al.*, 2004). A hydrosilylation approach towards formation of Si-C bonds on PSi, involving alkynes and alkenes, which yields surface bound vinyl and alkyl groups respectively has also been described (Zazzera *et al.*, 1997). The surfaces prepared through this route are remarkably stable to boiling alkali solutions, indicating that the degree of coverage is sufficient to fully protect the exposed surface. In contrast, the Si-H terminated PSi dissolves in minutes under these conditions (Buriak and Allen, 1998). Other treatments also included hydrosilylation of undecylenic acid (Boukherroub *et al.*, 2002; Wu *et al.*, 2011), in which the free carboxyl groups of undecylenic acid are covalently bonded on the surface and can be used to further surface functionalization; and the 3-aminopropyltriethoxysilane (APTES), where the molecule has been used as organometallic precursor (Arroyo-Hernandez *et al.*, 2006).

2.2.3 Biomedical applications

The discovery that PSi behaved as a bioactive material (Canham, 1995) instigated the scientific community in further pursuing PSi studies for biomedical applications. Reports on *in vitro* studies covering calcification (Canham, 1995; Canham and Reeves, 1996; Canham *et al.*, 1996; Rosengren *et al.*, 2000; Coffer *et al.*, 2003; Seregin and Coffer, 2006), cell adhesion and culturing (Bayliss *et al.*, 2000; Chin *et al.*, 2001; Sapelkin *et al.*, 2006), neural networks (Sapelkin *et al.*, 2006), protein adsorption (Collins *et al.*, 2002; Karlsson *et al.*, 2003; Karlsson *et al.*, 2004; Prestidge *et al.*, 2007; Prestidge *et al.*, 2008), and biodegradability studies (Canham *et al.*, 1999; Canham, 2000; Anderson *et al.*, 2003) have been published since. Also, some initial *in vivo* assessments of tissue compatibility have been carried out (Bowditch *et al.*, 1999; Rosengren *et al.*, 2000). Due to its large specific surface area and easily functionalized surface chemistry, PSi-based materials were further investigated in areas such as implantable devices (Santini *et al.*, 1999; Sharma *et al.*, 2006), biomolecular screening (Nijdam *et al.*, 2007; Nijdam *et al.*, 2009) and optical biosensing (Lehmann and Gösele, 1991; Palestino *et al.*, 2008). The possibility to fabricate optical multilayer structures not only enabled the use of PSi in optical sensor applications, but also in detecting changes in electrical, optical and photoluminescence properties

(Salonen and Lehto, 2008). The development of PSi materials for brachytherapy and for implantable drug delivery for the treatment of chronic eye diseases has already been given approval by the Food and Drug Administration (FDA). The PSi-based product Brachysil^{TM} of pSivida Ltd., the leading company in the biomedical applications of PSi, has already advanced to Phase II clinical trials for inoperable primary liver and pancreatic cancer (Zhang *et al.*, 2005; Goh *et al.*, 2007).

2.2.3.1 Biocompatibility and biodegradation

Biofunctionalization of the PSi surface is a crucial step considering potential *in vivo* applications. The surface chemistry should be designed in order to obtain the desired effects, and should be stable enough for the intended purpose, and yet displaying bioactivity. The first report on PSi biocompatibility came from Leigh Canham which investigated the growth of hydroxyapatite on top of the PSi in simulated body fluids (Canham, 1995). Subsequent studies showed several other remarkable properties of PSi such as high controllability, bio-inertness, bioactiveness, and resorbability (Canham, 2000; Arroyo-Hernández *et al.*, 2003). In addition to the biocompatibility, PSi biodegradation can also be controlled by the overall porosity, pore size, shape, surface and bulk properties (Canham, 1997; Decuzzi *et al.*, 2009), which in turn can be controlled by the choice of the material fabrication parameters (Anglin *et al.*, 2008; Tasciotti *et al.*, 2008). For instance, PSi with a porosity >70% dissolves in all the simulated body fluids (except gastric fluids), whereas PSi with a porosity <70% is bioactive and slowly biodegradable (Salonen *et al.*, 2008). Furthermore, macroporous Si is a rather bioinert material, as its bioactivity has also been showed to be dependent on the pore size (Canham *et al.*, 1996).

The fact that PSi degrades mainly into monomeric silicic acid, $Si(OH)_4$, the most natural form of Si in the environment and very important in human physiology in protecting against the poisonous effects of aluminium (Popplewell *et al.*, 1998), is an important feature that contributes even further to the PSi apparent biocompatibility. It has been reported that the average daily intake of Si in the Western World is approximately 20−50 mg/day (Jugdaohsingh *et al.*, 2002; Jugdaohsingh *et al.*, 2004) and that Si is an essential nutrient for the human body. Blood concentrations of $Si(OH)_4$ have been found to be slightly above the typical values of 1 mg/L (Popplewell *et al.*, 1998) and, most importantly, all $Si(OH)_4$ was shown to be efficiently excreted in urine (Bonanno and Delouise, 2010).

The PSi degradation from membranes into $Si(OH_4)$ and its impact on the biocompatibility of PSi in human ocular cells both *in vitro* and *in vivo*, in the rat eye has been evaluated. (Low *et al.*, 2009). Also, regarding ophthalmic applications, PSi encapsulated in microfibers of the biodegradable polymer polycaprolactone (PCL) was appraised, using both a cell attachment assay with epithelial cells and an *in vivo* assessment of biocompatibility in rats (Kashanian *et al.*, 2010). The study also assessed the surface chemistry of PSi dissolution kinetics, with the authors reporting that the composite material did not elicit any inflammatory response or infection. The covalent attachment of poly(ethylene) glycol (PEG) molecules to the PSi surface was also found to modulate the degradation kinetics of PSi structures (Godin *et al.*, 2010). Different molecular weight PEGs (245-5000 Da) were employed with the authors reporting that the *in vitro* degradation of the PEGylated particles (30–50 nm pores) in phosphate buffer solution

(PBS, pH 7.2) and serum at 37 °C showed slower particle degradation with increasing PEG molecular weight.

PSi has also been found to support living cultures of mammalian tissues. For example, adhesion of Chinese hamster ovary cells and rat hippocampal neurons (B50) (Sapelkin *et al.*, 2006), adhesion of rat pheochromocytoma (PC12, a neurosecretory cell line) and human lens epithelial cells (HLE) (Low *et al.*, 2006) and nerve tissue to PSi surfaces (Johansson *et al.*, 2009) have been already successfully demonstrated . Adhesion studies of PSi to biological surfaces have also shown the immunogenic effect of micro- and nanostructured Si-based surfaces for *in vivo* therapeutic or sensing applications. Ainslie and co-workers (Ainslie *et al.*, 2008) have studied the immune responses of four Si surfaces (nanoporous, microstructured, nanochanneled, and flat) in human blood derived monocytes after 48 h of exposure. They found that the immunogenicity and biocompatibility of flat, nanochanneled, and nano-PSi towards human monocytes were approximately equivalent to tissue culture polystyrene, and the formation of reactive oxygen species (ROS) was not found to be a prerequisite for inflammation in the Si-based surfaces.

The PSi prepared by electrochemical anodization of crystalline Si in HF-containing electrolytes, has been found to be a good reducing agent. Both the Si–H species on the surface and the skeleton consisting of elemental Si have reduction potentials sufficient to reduce many organic molecules (Wu *et al.*, 2011). This potential for generating highly reactive singlet oxygen from PSi particles in ethanol and aqueous media has been exploited for phototoxicity in cancer cells, leading to remarkable cell death in HeLa or NIH-3T3 cells (Xiao *et al.*, 2011). The *in vitro* cytotoxicity of PSi microparticles (1–75 μm) with different surface chemistries (TOPSi, TCPSi and THCPSi) in Caco-2 cells was reported to follow both concentration- and size-dependent trends (Santos *et al.*, 2010). The study showed that TOPSi surface chemistry induced a less pronounced cytotoxic response than TCPSi and THCPSi microparticles, and the suggested mechanisms of cytotoxicity included mitochondrial disruption, ATP depletion, ROS, and cell apoptosis. Together with its biocompatibility and the ability to yield harmless degradation products, the high surface area and high porosity of the PSi materials also raised the possibility to load drug compounds within its pores (Prestige *et al.*, 2007; Anglin *et al.*, 2008).

2.2.3.2 Drug delivery

The attainment of a controlled and localized release of drug compounds within the body is of paramount importance for increasing the efficacy and decreasing the potential side effects of therapy (Braeckmans *et al.*, 2002; Brigger *et al.*, 2002). The research over PSi-based materials for drug delivery applications emerged in the late 1990´s with reports of Si nanopore membranes (Desai *et al.*, 1999), although it became more prevalent after the year 2000 (Salonen and Lehto, 2008). One major advantage of the PSi materials is that they can be tailored for continuous or triggered drug release, depending on the application.

For example, PSi nanostructures can display responsive properties to chemical stimuli such as pH (Xue *et al.*, 2011). The loading of compounds into a PSi host can be carried out using different strategies, which can be grouped into the following general categories: covalent attachment, physical trapping and adsorption (Anglin *et al.*, 2008). The drug loading is affected by several factors involved in the process. These include pH

dependency, temperature, and time, but the most vital factor is the possible chemical reactivity of the drug loading solution with the PSi surface. Some drugs, like antipyrine, catalyze oxidation of the as-anodized PSi (Salonen *et al.*, 2005), and some other drugs, like ranitidine, strongly react even with TOPSi in methanol solution (Salonen *et al.*, 2008).

By combining the results of thermogravimetry and differential scanning calorimetry (DSC), the amount of drug confined within the pores of PSi determined (Lehto *et al.*, 2005). The thermodynamic states of ibuprofen loaded into PSi were also subsequently characterized using thermal analysis and nitrogen sorption (Riikonen *et al.*, 2009). The authors found three different thermodynamic states of ibuprofen in the samples: (1) a crystalline state in the surface outside the pores; (2) a crystalline state in the center of the pores; (3) and a disordered state between the pore wall and the crystalline core. The results supported the assumption of the existence of a layer of disordered ibuprofen adjacent to the pore wall (i.e., δ-layer) of around 2 nm, in which the thickness is not strongly dependent upon the pore size. Consequently, an increase in solubility and dissolution rate of the drug is achieved, as a result of the high lattice energy of the drug molecule inside of the pores (Yu, 2001; Huang and Tong, 2004). The tunable pore sizes and volumes were also found to control the amount of drug loaded within the pores and allow temporal release profiles (Anglin *et al.*, 2004). For example, six different types of PSi microparticles – as-anodized, TCPSi, TOPSi, annealed-TCPSi, annealed-TOPSi and THCPSi) – were prepared to evaluate the effect of the surface treatment and pore size on the dissolution properties and stability of PSi microparticles (Limnell *et al.*, 2007). It was observed that the hydrophilic TCPSi particles were the most stable and induced the fastest ibuprofen dissolution, and no changes in the release profiles of ibuprofen were observed after three months of stability testing (30 °C, 56% relative humidity).

The paracellular delivery of insulin across an intestinal Caco-2 cell monolayer using microfabricated PSi particles was one of the first examples of drug delivery using this material (Foraker *et al.*, 2003). The authors found that the permeation of insulin across Caco-2 cell monolayers was significantly enhanced and represented a 10-fold increase when compared with insulin delivered through oral formulations and up to 100-fold increase when compared with formulations without permeation enhancers. The release of the steroid dexamethasone from freshly etched, hydrogen-terminated PSi films was also found to be faster due to the chemical instability of PSi at physiologic pH, and the mechanism of drug release was suggested to be a combination between drug leaching and PSi matrix dissolution (Anglin *et al.*, 2004). Protein-conjugated microfabricated PSi systems for oral drug delivery have also been found to modulate the adhesion of these reservoir systems to the GI walls, potentially improving their drug delivering abilities (Ahmed *et al.*, 2002). In a study involving a two-layer PSi matrix with 2 µm pores and 200 nm thick layer loaded with doxorubicin (an anticancer drug), the authors found that the Si matrix exhibited a time-dependent drug release profile modulated by the thickness of the PSi layer (Vaccari *et al.*, 2006).

Studies involving TCPSi and TOPSi microparticles for oral administration have also been conducted using five model drugs: antipyrine, ibuprofen, griseofulvin, ranitidine and furosemide (Salonen *et al.*, 2005). The drug compounds were loaded into TCPSi and TOPSi microparticles and were investigated for their drug releasing behavior and stability in the presence of aqueous or organic solvents. The surface properties of the particles, the chemical nature of the drug and the drug loading solution, determined the compound

affinity towards the mesoporous particles' pores. The release rates of the loaded drugs from the TCPSi microparticles were also found to depend on the characteristic dissolution behavior of the drug substance in question: when the dissolution rate of the free/unloaded drug was high, the microparticles caused a delayed release. Another study concerning TCPSi microparticles loaded with furosemide, showed that both drug release/dissolution and permeation across a Caco-2 cell monolayer at pH values of 5.5, 6.8 and 7.4 were enhanced (Kaukonen *et al.*, 2007). The authors reported a 5-fold increase in furosemide permeation from the TCPSi-loaded particles when compared with the pre-dissolved drug.

Nanostructured TOPSi particles were also investigated for their effectiveness as drug carriers for sustained release of the antibacterial agent triclosan (Wang *et al.*, 2010). The study reported an enhanced inhibitory activity over a 100 day period. The same type of surface-treated particles was also used in order to improve the pharmacokinetic behaviour of indomethacin (IMC), a non-steroidal anti-inflammatory drug (Wang *et al.*, 2010). The dissolution profiles at pH 7.2 showed a rapid dissolution for both the IMC loaded in TOPSi particles and a commercial Indocid® formulation within the first 5 min (85 and 95 wt-% dissolved, respectively) compared to pure crystalline drug. The study also reported that the IMC plasma concentrations of fasted Sprague-Dawley rats showed significant increase in both C_{max} and bioavailability. Another study was conducted using two different strategies for loading doxorubicin: (1) physically adsorbed to PSi with 30–50 µm in size and 20–30 nm pore diameter, and (2) covalently attached to a 10-undecenoic acid linker, which was attached by thermal hydrosilylation and grafted to the PSi surface (Wu *et al.*, 2008). The authors reported that for the physically adsorbed drug, a rapid and complete drug release was observed within 24 h, whereas particles containing a combination of covalently attached and physioadsorbed doxorubicin displayed a gradual release over a period of > 24 h. In the case of the covalent attached doxorubicin, the drug was released only when the covalent bonds were broken or the PSi matrix was oxidized and degraded. The doxorubicin that was covalently attached to the particles showed a continuous and slower release for > 5 days. The drug release was proposed to be a two-step mechanism involving oxidation and subsequent dissolution of the PSi matrix.

Besides small molecules, peptide delivery from PSi materials has also been conducted.
The peptides Melanotan II (Kilpelainen *et al.*, 2011), ghrelin antagonist (Kilpelainen *et al.*, 2009), and PYY_{3-36} (Kovalainen *et al.*, 2011), human serum albumin (Zangooie *et al.*, 1998), papain and gramicidin A (Prestidge *et al.*, 2007; Prestidge *et al.*, 2008), have all been loaded into PSi and investigated both *in vitro* and *in vivo*. For example, the *in vitro* release of the protein papain from PSi powders has shown both a burst and sustained release depending on the PSi surface modification and loading degree (Prestidge *et al.*, 2007). Importantly, the interactions between the PSi surfaces and the loaded peptides/proteins were found to be crucial and to define the success of loading and/or release from the particles. Other authors loaded an antibiotic (vancomycin) into PSi films and trapped the peptide by capping the films with a layer containing bovine serum albumin (BSA), in order to obtain a pH-triggered release system (Perelman *et al.*, 2008). At pH 4.0 the drug was not released from the films of different thicknesses, whereas when the pH was increased to 7.4, BSA was dissolved and vancomycin was released into the solution. TOPSi surfaces were also shown to effectively control protein interactions, which dictate adsorption, protein structure, and bioactivity (Jarvis *et al.*, 2010). Adsorption mechanisms of lysozyme, papain, and human serum albumin were shown to be controlled by both protein structure and PSi surface chemistry, via hydrophobic interactions and electrostatic

attractions. High protein adsorption onto unoxidized PSi (240–610 μg/m^2) was attributed to predominately hydrophobic interactions, which resulted in structural changes of the adsorbed proteins and significant loss of bioactivity.

2.2.3.3 Cellular interactions

When nanoengineered carriers are administered in the body, they encounter several physiological barriers and interact extensively with the cellular environment. Throughout their translocation the particles will encounter a number of the organism's defenses that can eliminate, sequester, or dissolve the particles. In addition, cells and tissues have effective antioxidant defenses that deal with ROS generation (Figure 2). The hierarchical oxidative stress model hypothesizes that materials can elicit different types of responses at different levels that might even not be cytotoxic, but nonetheless represent an aggression to the cell (Nel *et al.*, 2006). The first tier of response to the foreign material involves the anti-oxidant defense pathway, which leads to the activation of the nuclear factor (erythroid-derived 2)-like 2 (Nrf-2), responsible for the expression of various genes including those encoding several antioxidant enzymes. The final outcome of this pathway is the activation of Phase II enzymes, which are responsible for conjugation reactions and usually detoxicating in nature. The second tier of response regards to the eliciting of inflammatory reactions, with the activation of the redox-sensitive transcriptor factors, nuclear factor kappa B (NF-κB), a key regulator of immunity, inflammation and cell proliferation which also regulates the mitogen activated protein (MAP) kinase pathway (Müller *et al.*, 1997) and the activator protein 1 (AP-1), also responsible for apoptosis (Ameyar *et al.*, 2003). The activation of these transcription factor leads to final release of chemokines and cytokines in the body. The final tier of aggression might result in cytotoxicity involving the mitochondrial permeability transition pore (PT pore), an opening in the mitochondrial membrane which results in a sudden permeability increase of the inner mitochondrial membrane to solutes and some proteins, thereby disrupting the inner transmembrane potential. The PT pore might be accompanied by colloidosmotic swelling and uncoupling of oxidative phosphorylation, as well as by the loss of low molecular weight matrix molecules such as calcium and glutathione. The outcome of this cascade of phenomena that occur when the cytotoxic path is activated is apoptosis, or programmed cell death (Trachootham *et al.*, 2008).
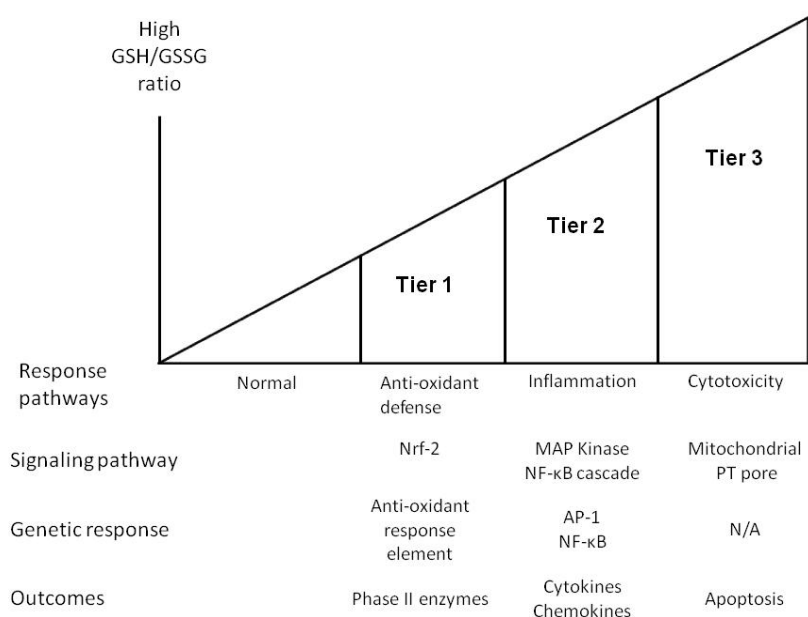
Figure 2   *Schematic diagram of the hierarchical oxidative stress mode. Modified from Nel et al., 2006. Copyright © (2006) AAAS. Reprinted with permission.*

The thorough list of all cellular models tested with Si materials is quite extensive but nonentheless, some studies conducted have been of special interest in the field. A report on the p-type, flat, nanoporous, micropeaked and nanochanelled Si surfaces in contact with a human blood monocyte model, regarding cytokine and chemokine analysis as well as ROS assessment and cytotoxicity, has showed that the immunogenicity and biocompatibility of the PSi surfaces towards human monocytes is approximately equivalent to tissue culture polystyrene (Ainslie *et al.*, 2008). Also, relating to the generation of ROS, other authors have reported that as-anodized PSi microparticles produced ROS, which interacted with the components of the cell culture medium, leading to the formation of cytotoxic species (Low *et al.*, 2010). The oxidation of PSi microparticles not only mitigated, but also abolished any toxic effects. Furthermore, several reports on cell adhesion of PSi wafers have also been published (Bayliss *et al.*, 1999; Bayliss *et al.*, 2000; Sapelkin *et al.*, 2006), consistently showing that silicon substrates are not toxic to the cells, which remain viable in terms of respiration and cell membrane integrity.

PSi particles have revealed their drug delivering potential by exploring the possibility to assemble in multistage delivery devices. The development of PSi microparticles as a multistage delivery system loaded with one or more types of second stage particles has been given substantial attention by Prof. Ferrari's group (Tasciotti *et al.*, 2008; Serda *et al.*, 2010; Tanaka *et al.*, 2010; Godin *et al.*, 2011). This technology relies on biodegradable stage 1 microparticles (S1MPs) composed of lithographically engineered PSi with defined shapes, sizes and porosities (Serda *et al.*, 2009; Chiappini *et al.*, 2010) which enables them to attain optimal margination, firm adhesion, and tunable internalization properties (Decuzzi *et al.*, 2005; Decuzzi and Ferrari, 2008; Decuzzi *et al.*, 2009). The S1MPs can be subsequently loaded with several types of other smaller particles or stage 2 nanoparticles. (S2NPs). The hemispherical shape of these carriers was found to be beneficial in terms of

margination towards the vasculature wall in circulation, biodistribution, endothelial adhesion, and cell internalization when compared with spherical carriers (Decuzzi *et al.*, 2004). These rationally-designed carriers were further employed in personalized targeting, overcoming barriers such as enzymatic degradation, vascular endothelium crossing, and molecular efflux pumps. The ability of these logic-embedded vectors to surmount biological barriers, such as cellular membranes, hemorheology, and reticuloendothelial system (RES) uptake was confirmed in a number of studies by the same group (Serda *et al.*, 2009; Serda *et al.*, 2009; Godin *et al.*, 2010). Preclinical studies on the quasi-hemispherical and discoidal PSi particles with dimensions of 600 nm–3.2 µm (Chiappini *et al.*, 2010) have shown that the PSi microparticles are phagocytosed by vascular endothelial cells (Serda *et al.*, 2009; Serda *et al.*, 2009; Serda *et al.*, 2009), and accumulate mainly in phagosomes (Serda *et al.*, 2009). The main advantage of these systems is that they can be loaded with many different agents, such as proteases, contrast agents, siRNA, and therapeutic genes, rendering them a very versatile platform for drug delivery and imaging purposes.

The cell morphology and function was also shown to be greatly influenced by both the substrate surface characteristics and the presence of a 3D collagen mesh in PC12 cells (Lopez *et al.*, 2006). Other authors (Alvarez *et al.*, 2009) studied the attachment and viability of primary cells with PSi films of various surface chemistries (SiO$_2$, decyl, undecanoic acid, and oligoethylene glycol), and evaluated their ability to retain optical reflectivity properties relevant to molecular biosensing. The hepatocytes were found to adhere better to surfaces coated with collagen and chemical modification of PSi did not affect the rat cells. In addition, the PSi samples hydrosilylated with a hydrophilic, carboxylic acid species (collagen-coated undecanoic acid modified) showed the best stability and compatibility with primary rat hepatocytes, similar to those observed for standard culture preparations on tissue culture polystyrene.

A study using an electrospinning method to produce 3D-fibrous structures of PSi/PCL for orthopedic purposes has found that the highly porous and slowly degrading PSi/PCL micro-fibrous scaffolds supported human mesenchymal stem cells and bone marrow-derived mouse stromal cells in their ability to proliferate, migrate, and differentiate (Fan *et al.*, 2011).

2.2.3.4 Protein coating

Besides the advantages described above, PSi surfaces can made even more biocompatible and chemically stable by self-assembling a biofilm of proteins, such as hydrophobins, (HFBs) onto its surface (De Stefano *et al.*, 2007; De Stefano *et al.*, 2008; De Stefano *et al.*, 2009). Hydrophobins are a family of surface active proteins of fungal origin that have the ability to form self-assembled layers on hydrophobic materials and modify the surface binding properties, thus turning hydrophobic surfaces into hydrophilic (Hektor and Scholtmeijer, 2005; Linder, 2009; Laaksonen *et al.*, 2010; Varjonen *et al.*, 2011). As a result, the wettability properties of PSi can be altered (De Stefano *et al.*, 2009), leading to the production of a chemically and mechanically stable homogenous monolayer of self-assembled proteins with improved characteristics in terms of surface interaction. In addition to the efficient dispersion in aqueous media of nanomaterials such as single-walled carbon nanotubes (Kurppa *et al.*, 2007) or Teflon[®] powders (Lumsdon *et al.*, 2005), these

proteins have also been reported to stabilize drug nanoparticles by acting as surfactants improving the dissolution of water insoluble drugs (Akanbi *et al.*, 2010; Valo *et al.*, 2010) and for drug immobilization on nanofibrilar cellulose using an HFB engineered variant (Valo *et al.*, 2011). The ability to modulate protein adhesion and wettability in the HFB-coated surfaces (Hektor and Scholtmeijer, 2005), suggests the possibility to modify the interaction of PSi surfaces with endogenous proteins when administered in the body (Sarparanta *et al.*, 2011). Furthermore, the HFB was also found to play a role in the prevention of host immune response to fungal spores (Aimanianda *et al.*, 2009), leading to the hypothesis that these proteins could confer shielding against immune-system recognition *in vivo*.

Following *in vitro* testing, the *in vivo* assessment of a potential drug carrier is crucial in order to understand the pharmacodynamics and biodistribution of such carrier and anticipate its harmful reactions. The accumulation and clearance of nanoparticulate systems are also critical parameters to address when such carriers are envisioned to be translated to the clinic.

2.2.3.5 Biodistribution, accumulation and clearance

Although essential, biodistribution studies concerning PSi particles have been scarce so far. From the several reports already published regarding *in vivo* PSi testing, most deal with PSi microparticles and implants (Table 3).

Table 3   *Type of PSi materials used for in vivo studies and type of analysis conducted. Adapted from Santos et al., 2011.Copyright © (2011) Bentham Science Publishers. Reprinted with permission.*

Material type	*In vivo* model	Aim	Reference
p-type, thermally oxidized and thermal hydrosililyzed 1-270 μm particles	Rabbit eye vitreous	Particle degradation and cytotoxicity	(Cheng *et al.*, 2008)
boron-doped, 50 and 200 nm ultrasonicated PSi particles	A20 and A20-grafted Balb/c mice	increase peptide bioavailability, targeting enhancement and cytotoxicity	(De Angelis *et al.*, 2010)
p^{++}-type, 1.6×1.6 μm semi-spherical, 1.6×0.3 μm discoidal and 1×1 μm cylindrical PSi particles	MDA-MB-231-grafted nu/nu nude mice	Biodistribution, size and shape dependency	(Decuzzi *et al.*, 2010)
^{32}P-Brachysil™ 20 μm microparticles	human clinical trial – hepatcellular carcinoma	Safety, tolerance and anti-tumor efficacy	(Goh *et al.*, 2007)
p-type 200 μm pSi–PCL electrospun fibers	HLE and Sprague–Dawley rats	Dissolution kinetics, attachment, in vivo ocular inflammation and neovascularization	(Kashanian *et al.*, 2010)
p^{+}-type, THCPSi 38-53 μm particles	Wistar rats and Balb/c mice	Peptide (Ghrelin antagonist) release, effect on blood pressure, food intake and cytokine release	(Kilpelainen *et al.*, 2009)
p^{+}-type, THCPSi 38-53	Wistar rats and	Peptide (Melanotan II)	(Kilpelainen

μm particles	Balb/c mice	release, effect on heart rate and water intake	*et al.*, 2011)
n-type, TOPSi and TOPSi-aminosilanised 1-60 μm membranes	HLE, human corneal cells and Sprague–Dawley rats	Biocompatibility, dissolution and cellular growth	(Low *et al.*, 2009)
p^{++}-type, 130-180 (126) nm biopolymer-coated PSi particles	MDA-MB-435 and MDA-MB-435 grafted-BALB/c mice	Degradation, cytotoxicity, drug (doxorubicin) release, biodistribution, in vivo imaging	(Park *et al.*, 2009)
p-type, plane and PSi 4×4×0.5 mm implants	Rat (abdominal wall)	Capsule formation, thickness and immunoreactivity	(Rosengren *et al.*, 2000)
p^{++}-type, 1.6 μm diameter APTES-modified, targeted-liposomal siRNA loaded PSi particles	HeyA8-Lc and Skov3ip1-Lc and NCr-nu mice	Biodistribution, biodegradation, sustained targeted siRNA delivery, *in vivo* protein knockdown, cell proliferation and tumor growth	(Tanaka *et al.*, 2010)
p$^+$-type, 13.6 μm TOPSi particles	Sprague-Dawley rats	Drug (indomethacin) release, *in vivo* absorption, *in vitro-in vivo* correlation (IVIVC)	(Wang *et al.*, 2010)
p^{++}-type, 1.6 μm diameter oxidized negatively charged and APTES-modified positively charged PSi particles	FBV mice	Cytotoxicity, cytokine release, tissue accumulation, renal and hepatic function	(Tanaka *et al.*, 2010)
^{32}P BioSilicon™	HepG2 and 2119 grafted-BALB/c mice	Time-response tumor volume, histology	(Zhang *et al.*, 2005)

One of the pioneering reports of luminescent PSi nanoparticles (LPSiNPs) prepared by electrochemical etching of single-crystal Si wafers for *i.v.* delivery was first published in 2009 by the group of Prof. Sailor (Park *et al.*, 2009). The authors fabricated PSi particles under 200 nm in size and then loaded them with doxorubicin. They were able to demonstrate that the drug was slowly released under physiological conditions, reaching a maximum within 8 h and that no significant toxicity could be related to the degradation product of the material in the animal tissues. When mice were injected *i.v.* with suspensions of the nanoparticles (20 mg/kg), they were able to clear the particles from the body within 4 weeks. Interestingly, such system was also demonstrated to be suitable for *in vivo* imaging after intra muscular and sub-cutaneous injections in nude mice. The monitoring of the particles by near-infrared fluorescence showed that the adsorption of a dextran layer onto the surface of the particles with 126 nm in diameter, pore diameters of 5−10 nm and a zeta potential of –52 to –39 mV, increased the stability of the material, allowing better and longer-lasting visualization in the animal body after administration. The biodistribution and histological studies in mice 24 h after injections showed that the LPSiNPs particles accumulated preferentially in the spleen rather than in the liver, whereas the dextran-coated LPSiNPs accumulated more in the liver than in the spleen. The injection of the dextran-coated LPSiNPs into the nude mice bearing a tumor led to an accumulation of the nanoparticles in the tumor, aiding its visualization.

A report on the biocompatibility and safety of *i.v.* administered PSi structures with a diameter of 1.6 μm and pore size of 36 nm, negatively (−32 mV) and positively (8.7 mV) charged, after acute single doses (10^7, 10^8, 5×10^8 PSi particles/animal) and subchronic multiple doses (10^8 PSi particles/animal/week for 4 weeks) in immunocompetent mice was

subsequently published (Tanaka *et al.*, 2010). In this study, discoidal-shaped particles were used (Ferrari *et al.*, 2011), and the histopathological evaluation revealed that the PSi particles accumulated primarily in the liver and spleen with no indication of leukocyte infiltration. No significant innate or adaptive inflammatory responses were observed following either the acute or sub-chronic administration. Furthermore, the PSi particles did not change plasma and lactate dehydrogenase (LDH) levels of renal and hepatic biomarkers, as well as of 23 plasma cytokines, which showed that the particles were well tolerated both in single and sub-chronic multiple administrations. Another study concerning the biodistribution of quasi-hemispherical, discoidal and cylindrical particles after intravascularly injection into tumor-bearing mice was also published (Decuzzi *et al.*, 2010). The authors demonstrated that for the quasi-hemispherical beads, the number of particles accumulating in the non-RES organs reduced monotonically as the diameter of the particles increased, suggesting the use of smaller particles to provide a more uniform tissue distribution. However, discoidal particles have also been observed to accumulate more than others in most of the organs but the liver, where cylindrical particles are deposited in a larger extent. The use of near-infrared imaging for non-invasive *in vivo* assessment of the biodistribution of nanoporous discoidal Si particles has also been employed, suggesting that particles predominantly accumulated in the liver and spleen after 24 h (Tasciotti *et al.*, 2011). Proteomic analysis of intravascularly injected cationic and anionic discoidal PSi particles showed that cationic microparticles displayed a 25-fold greater abundance of immunoglobulin light variable chain, fibrinogen, and complement component 1 compared to their anionic counterparts. The anionic microparticles were found to accumulate equally in murine liver and spleen, whereas cationic microparticles showed preferential accumulation in the spleen (Serda *et al.*, 2011). Immuno-histochemistry supported macrophage uptake of both anionic and cationic microparticles in the liver, as well as evidence of association of cationic microparticles with hepatic endothelial cells. Particulate systems have different stability, behaviour in the biological microenvironment, and cellular distribution according to their size, morphology and chemical constitution (Moghimi *et al.*, 2005). Even at a nanoscale, biological compounds will interact very differently with the cellular environment compared with non-biological compounds such as metals, metalloids or synthetic polymers (De Jong and Borm, 2008). Therefore, a thorough understanding of particle-cell interaction should be developed before a drug carrier can come into the clinical setting.

Safety and biocompatibility of PSi engineered structures are, therefore, a requirement both in manufacture and, more importantly, when *in vivo* exposure or administration is concerned. In this context, there are several different responses that these nanoengineered materials may induce when in contact with cells. Consequently, a full characterization of the toxicological issues regarding these structures is crucial in the pre-clinical stage. Furthermore, even when all *in vitro* studies are conducted, a thorough understanding on the biodistribution of these materials is critical in order to validate them as potential drug carriers and to envision their human application.

3 Aims of the study

The aim of this thesis was to investigate the biocompatibility of PSi particulates with different cell models and to biofunctionalize the PSi surface with a self-assembled functional protein coat.

The specific objectives of this study were:

1. To address the biocompatibility, inflammatory response, oxidative stress and drug permeation properties of thermally oxidized PSi particles (**I**).

2. To investigate the biocompatibility, inflammatory response and oxidative stress of thermally hydrocarbonized PSi particles, as well as to evaluate thes biodistribution in a rat model (**II**).

3. To develop a method for reproducibly coat thermally hydrocarbonized PSi microparticles with a self-assembling hydrophobin class II (HFBII) protein and to investigate their biocompatibility and drug release properties (**III**).

4. To characterize HFBII-coated thermally hydrocarbonized PSi nanoparticles in terms of their biocompatibility and cellular association, as well as to investigate their drug permeation properties (**IV**).

5. To assess the gastro-retentive properties of HFBII-coated thermally hydrocarbonized PSi nanoparticles and their biocompatibility in a gastric cell line (**V**).

4 Experimental

Detailed descriptions of the methods, suppliers of the materials and the equipment used in this work can be found in the respective original publications (**I-V**). The PSi-based materials (**I-V**) were produced at the Laboratory of Industrial Physics, Department of Physics and Astronomy, University of Turku. The radiolabelling of the particles and HFBII, and the animal experiments (**II**, **IV** and **V**) were conducted at the Laboratory of Radiochemistry, Department of Chemistry, University of Helsinki.

4.1 Materials and methods

4.1.1 Mesoporous silicon particles (I-V)

The PSi particles were prepared from boron doped monocrystalline Si wafers $\langle 100 \rangle$ of p+-type with resistivity values of 0.01−0.02 Ωcm. The anodization of the wafers was done in a 1:1 (v/v) HF (38%)−ethanol (EtOH) mixture in a Teflon® container. For the microparticles (**I**, **II** and **III**), the free-standing films were obtained by etching the wafer for 40 min using a constant current density (50 mA/cm^2) followed by the detachment of the porous film from the substrate by abruptly increasing the current density to the electropolishing region. The films were then dry milled in a high energy ball mill system for a short period in an agate grinding jar, after which they were dry sieved repeatedly in mesh sieves until the desired size fractions were obtained. Each fraction of the microparticles was then wet sieved with absolute EtOH to separate the larger aggregates and dried at 65 ºC.

For the nanoparticles, the electrochemical etching consisted of the application of three different current pulses: (1) a first low current pulse to produce a mesoporous structure; (2) a second shorter pulse near the electropolishing region, which produced highly porous and mechanically fragile layers; and (3) a third zero-current pulse to remove the possible electrolyte concentration gradients in the pores formed during the high current pulse, before a new etching cycle starts. Finally, an increase in the current intensity near the electropolishing region was used in order to separate the multilayer film from the substrate.

4.1.1.1 Particle surface treatments (I-V)

The as-anodized hydrogen terminated surface of PSi is prone to oxidation, and therefore, needs to be surface treated in order to be stabilized. Before the surface stabilization, all particles were either mesh sieved (microparticles) or wet-sieved and centrifuged (nanoparticles) to the desired size fractions. From the surface treatments that can be employed for the stabilization of the particles, the thermal oxidation (**I**) and the thermal hydrocarbonization (**II-V**) were utilized and studied in this dissertation. With the exception of thermally oxidized particles, prior to any surface treatment, all the sieved particles were immersed in HF in order to remove the surface oxide formed during the milling. For the thermal oxidation , the temperature treatment consisted in exposing the particles to 300 ºC

for 2 h at ambient air. The particles obtained in this fashion, TOPSi, have oxidized terminated Si-O bonds and are hydrophilic. The thermal hydrocarbonization treatment consisted of exposing the particles to a 1:1 (v/v) flow mixture of N_2 and acetylene for 15 min at room temperature, followed by 15 min at 500 ℃, and then cooling down to room temperature under a N_2 flush. This type of treatment protects even further the particles, THCPSi, against oxidation, but on the other hand, yields very electrostatic particles, with hydrophobic Si-C-H terminated bonds.

4.1.1.2 Particle drug loading (I, III and IV)

The drugs were loaded into the pores of the PSi particles using an immersion method. This method consisted in dissolving the drug model compounds, griseofulvin (**I**) and IMC (**III** and **IV**), in an appropriate solvent at the following concentrations: griseofulvin (**I**) 75 mg/mL in dichloromethane (DCM) and IMC 175 mg/mL in dimethylsulfoxide (DMSO; **III** and **IV**). The loading was carried out at room temperature for both griseofulvin and IMC with a ratio of 0.5 mL of drug solution to 15 mg of particles and 0.5 mL of drug solution to 85 mg of particles, respectively. The loading time was 3 h, after which the particles were centrifuged and the excess of loading solution removed. The griseofulvin-loaded particles were dried at 65 ℃ at atmospheric pressure and the IMC-loaded particles were vacuum filtered from the loading solution at 40 ℃ under vacuum (< 2 mbar).
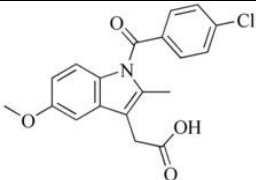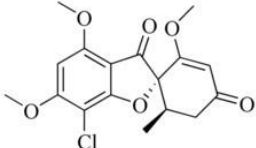
4.1.1.3 Particle ^{18}F-radiolabelling (II and V)

Fluorine-18 was produced in a $^{18}O(p,n)^{18}F$ reaction on a IBA Cyclone 5/10 cyclotron. To 1 mg of THCPSi nanoparticles suspended in anhydrous dimethylformamide (DMF) it was added 500 µL of 4% (v/v) acetic acid and 0.5−1 GBq of fluorine-18 as [^{18}F]KF/Kryptofix 2.2.2 in 100 µL of DMF. The solution was then heated at 120 ℃ for 15 min. The radiolabeled nanoparticles were purified with sequential washes in absolute ethanol, ultrapure water and 1×Hank's Balanced Salt Solution (HBSS, pH 7.4). The particles were then centrifuged at 29,000 *g*, the supernatant was changed and the particles were re-suspended by sonication between washes. The final formulation was prepared in 5% Solutol-1×HBSS (pH 7.4).

4.1.2 Model drug compounds (I, III and IV)

Model drug compounds used in the studies were griseofulvin (**I**) and IMC (**III** and **IV**). The chemical structures and physicochemical properties of the drugs are depicted in Table 4. The drugs tested are similar in molecular weight and pKa, and are both poorly soluble but highly permeable compounds (Biopharmaceutical Classification System II).

Table 4   *Properties and structures of the model drug compounds (I, III and IV).*

Drug compound	Structure	Molecular weight	pK$_a$	Publication
Indomethacin (IMC)		357.8	4.5	**III, IV**
Griseofulvin		352.8	4.4	**I**

4.1.3 Hydrophobin II coating (III-V)

The Hydrophobin II (HFBII) was first purified from the culture supernatant of a *Trichoderma reesei* cultivation and purified by surfactant extraction (Linder *et al.*, 2001). For the coating of THCPSi with HFBII (**III**-**V**), a HFBII solution (0.5−1 mg/mL) was prepared in a glass tube using McIlvane's buffer (pH 4.0) as a solvent. Empty or drug-loaded particles were then added to the HFBII solution at a mass ratio of 4:1 (particle/HFBII) and gently stirred for several minutes until the particles were dispersed in solution, followed by an incubation at 80 ℃ for 30 min. The solution was then centrifuged at 6,000 *g* for 2 min and the entire supernatant removed. The particles were then washed four times with 1 mL of ultrapure water with subsequent centrifugation cycles at 6,000 *g* for 2 min for every wash. The particles were then dried at 60 ℃ and were either re-suspended in ultrapure water, HBSS or used as a dry powder. The quantification of HFBII protein was carried out using the bicinchoninic acid (BCA) assay (**III**-**V**) or high performance liquid chromatography (HPLC; **IV** and **V**).

4.1.3.1 HFBII ^{125}I-radiolabelling (IV and V)

The HFBII was radiolabeled with ^{125}I in 10^{-5} M NaOH (pH 8-10 reductant-free) using a standard procedure for radioiodination with the Bolton-Hunter method (Bolton and Hunter, 1973). The N-succinimidyl-3-(hydroxyphenyl)propionate (SHPP) was synthesized from 3-(4-hydrophenyl)propionic acid and N-hydrosuccinimide. The purity of SHPP-^{125}I was then verified with thin layer chromatography (TLC) on a 60 F$_{254}$ plate developed with 9:1 (v/v)

ethyl acetate-methanol. A volume of 50 µL of 1mg/mL of HFBII in 100 mM sodium-borate buffer, (pH 8.5) was added to the dried SHPP-^{125}I and the reaction mixture was incubated at 40 ℃ for 45 min. The HFBII-^{125}I was subsequently purified on a G-25 column preconditioned with 8 mL of McIlvane buffer (pH 4.0). The product was eluted with 3 mL of the buffer collecting 200 µL fractions. The fractions were measured on a dose calibrator and peak fractions pooled. A 0.2-µL sample from the pooled peak fractions was spotted on a chromatography paper and developed with 50:50 (v/v) methanol−water for determination of radiochemical purity of HFBII-[125]I. The TLC plate and chromatography paper were subsequently exposed to a digital imaging plate for 48 h. The imaging plate was scanned on a scanner and the autoradiographs analyzed with imaging software. Immediately after pooling, 0.1 mg of HFBII carrier in McIlvane buffer (pH 4.0) was added to the HFBII-^{125}I solution to prevent adsorption to the vial walls. The HFBII was quantified against a standard series by HPLC.

4.1.4 Cell culture (I-V)

Human colon adenocarcinoma Caco-2 (**I-IV**), Human gastric adenocarcinoma AGS (**III** and **V**), human colorectal adenocarcinoma HT-29 (**III** and **IV**) and murine macrophage RAW 264.7 (**II**) cells were all obtained from American Type Culture Collection. All cell types, except AGS, were grown in a medium consisting of Dulbecco's Modified Eagle Medium (DMEM; 4.5 g/L glucose) supplemented with 10% fetal bovine serum (heat-inactivated at 56 ℃ for 30 min), 1% non-essential amino acids, 1% L-gutamine (200 mM), penicillin (100 UI/mL), and steptomycin (100 µg/mL). AGS cells were cultured in the same conditions, but the medium used was Roswell Park Memorial Institute (RPMI) 1640 medium. The cells were maintained at 37 ℃ in an incubator at an atmosphere of 5% CO_2 and 95% relative humidity. The growth medium was replaced three times a week during cell growth and differentiation.

Prior to each experiment, the cells were harvested using a 0.25% (v/v) trypsin-Ethylenediaminetetraacetic acid-PBS solution and then seeded at the desired cell density. For the reactive oxygen species (ROS; **I** and **II**), nitric oxide (NO; **I**), tumor necrosis factor α (TNF-α; **I** and **II**) and viability assessment (**I-V**), 100 µl of cells were seeded at a density of 2×10^5 cells/mL in 96-well plates in DMEM or RPMI 1640 and allowed to attach overnight. For the permeability studies (**I-IV**) and transmission electron microscopy (TEM) flat embedding using Caco-2 (**I**), 500 µl of cells in DMEM were seeded in 12-Transwell® cell culture inserts at a density of 1.5×10^5 cells/mL. The medium was changed three times a week and the cells for the permeation studies were used between 21 and 28 days after seeding. For the TEM flat embedding of RAW 264.7 macrophages (**I**), 3×10^4 cells in DMEM were seeded on top of a 13 mm glass round cover slip placed at the bottom of each 12-well plate. For the confocal fluorescence microscopy (**II**, **IV** and **V**), 200 µl of cells in DMEM at a density of 1×10^7 cells/mL were seeded in a 8-well chambered No. 1 borosilicate coverglass system plate (**II**) or 1 mL of cells in DMEM or RPMI at a density of 2×10^5 cells/mL were seeded on top of a 13 mm glass round cover slip placed at the bottom of a 12-well plate (**IV** and **V**). For the flow cytometry measurements, 1 mL of cells in DMEM or RPMI at a density of 2×10^5 cells/mL was seeded in a 12-well plate (**IV** and **V**).

4.1.5 Dissolution media and other chemicals (I-V)

The HBSS buffer was used as a medium for the drug release (**III**) and drug permeation (**I-IV**) studies, and ROS (**I and II**), NO (**I**), TNF-α (**I and II**) and viability assays (**I-V**). Biological buffers [4-(2-hydroxyethyl)piperazine-1-ethanesulfonic acid] (HEPES) or [2-(N-morpholino)ethanesulfonic acid] (MES) at 10 mM concentration were used to buffer the HBSS solutions to pH 7.4 and 5.5 (**I-V**) respectively. A mixture of 0.2 M HCl/ 0.2 M KCl was used as the pH 1.2 buffer. For the preparation of fasted state simulated intestinal fluid (FaSSIF) (**I**), NaOH pellets, glacial acetic acid and NaCl were used in purified water and the pH adjusted to 6.5.

Solvents used in the manufacturing of the particles, HPLC analysis and drug loading/release quantification were EtOH (**I-V**), phosphoric acid (**I-V**), acetonitrile (**I, III and IV**), DCM (**I**) and DMSO (**III and IV**). A solution of D-[^{14}C]mannitol was also used to assess the Caco-2 monolayer integrity after the permeation studies (**II**).

4.2 Analytical methods

4.2.1 Physical methods (I-V)

The DSC was carried out at heating rates of 10 ºC/min under a N_2 gas purge with a flow rate of 40 mL/min in order to detect crystalline fractions of the drug on the surface of the particles after loading (**I and III**). The porous properties of the particles were studied using N_2 ad/desorption (**I-V**). The surface areas and pore characteristics of the particles were determined from the obtained data using the Brunauer-Emmet-Teller (BET) and Barret-Joyner-Halenda (BJH) methods, respectively. Fourier transform infrared spectroscopy (FTIR) was used to evaluate chemical changes in the particle samples, as well as possible residual solvents after loading, coating or surface treatment (**II, III and IV**). The particle morphology was evaluated both from scanning electron microscopy (SEM) (**I and III**) and TEM images (**I, II and IV**). The cellular interactions were also evaluated using TEM images (**I**). The cellular association of fluorescently labeled particles was further evaluated using confocal fluorescence microscopy and flow cytometry (**II, IV and V**). Nanoparticle size distribution was also analyzed using a laser diffraction instrument (**I, II, IV and V**). The zeta (ζ)-potential of the nanoparticles (**I, II, IV and V**) was measured by a Zetasizer® instrument and calculated from the measured electrophoretic mobility using the Schmolukovski equation.

4.2.2 Compound quantification (I, III-V)

The concentration of the model compounds in the drug release, drug permeation, loading degree experiments and HFBII quantification were analyzed by HPLC and BCA. Detailed description of the HPLC experimental setup and conditions used can be found in the respective original publications (**I, III-V**). For the determination of [^{14}C]mannitol, 100 µL samples were mixed with 4 mL of scintillation cocktail and the [^{14}C]-activity was determined in each sample using a Liquid Scintillation Counter (**II**).

4.3 *In vitro* biocompatibility studies (I-V)

The *in vitro* biocompatibility studies comprised ROS, NO, TNF-α and fluorescence-based and luminescence-based cell viability assays. The cell culturing media and seeding procedures are described in chapter 4.1.4. The assays were conducted in 96-well plates after removing the culture media and washing the wells twice with HBSS (pH 7.4). All particles were dispersed in HBSS (pH 7.4) prior to the addition to the cell-containing wells and incubated with the cells for the desired exposure time. All assays were conducted at least in triplicate ($n \geq 3$).

4.4 Drug release experiments (III)

The dissolution media used in the drug release experiments are described in chapter 4.1.5. The experiments were carried out using a paddle dissolution method at 100 rpm at 37 °C as described in the European Pharmacopoeia. The volume of the media used was 500 mL at pH 1.2, 5.5 and 7.4, and all experiments were conducted under sink conditions. The IMC-loaded THCPSi particles and the bulk IMC were weighed and placed in the dissolution glass vessels and the dissolution media added afterwards. During the drug release studies, 1 mL aliquots were collected at the selected time intervals for quantification of the released/dissolved drug compound. The HPLC quantifications of the total amount of drugs loaded into the particles were carried out by weighing 1-3 mg of particles in 10 mL of pure DMSO, followed by adding 3 mL of EtOH. The mixtures were then vigorously stirred for 5 h and the amount of released drug was quantified from the liquid fractions by HPLC.

4.5 Permeability experiments (I-IV)

The permeability of a fluorescein isothiocyanate (FITC)-labeled particles (**II**), griseofulvin (**I**) and IMC (**III** and **IV**) across differentiated Caco-2 cell monolayers (**I-IV**) in an apical-to-basolateral direction was carried out using an apical pH of 5.5 and 7.4, and a basolateral pH of 7.4. Prior to all permeability experiments the cells were rinsed twice with HBSS (pH 7.4) and then equilibrated in the transport buffers under the experimental conditions for 30 min. The transepithelial electrical resistance (TEER) was measured prior to the experiments in order to confirm the integrity of the differentiated cell monolayer. Monolayers with TEER values above 250 Ωcm^2 were considered acceptable for the studies. The FITC-labeled THCPSi particles (**II**) in HBSS (pH 7.4) were introduced into the apical compartment and basolateral samples were collected at the selected time intervals, with the sample volume withdrawn replaced by fresh HBSS (pH 7.4). The samples were then analyzed for fluorescence and compared with the initial fluorescence values from the apical side. Griseofulvin was introduced into the apical compartment (**I**) either as a bulk powder or loaded into the TOPSi particles at pH values of 5.5 and 7.4. The samples were collected as described for the FITC-labeled THCPSi particles, but in this case the griseofulvin analysis was carried out by HPLC. Bulk IMC and the IMC-loaded into uncoated or HFBII-coated THCPSi microparticles (**III**) at pH values of 5.5 and 7.4 was also analyzed as described previously for griseofulvin. All permeability experiments were conducted at least in triplicate ($n \geq 3$).

The differentiated monolayer integrity was controlled after each permeability experiment by two methods. First, the cells were washed once with HBSS at the experimental pH and the TEER values were measured (**I-IV**). In addition, the monolayer integrity was further assessed after the drug permeability tests with [^{14}C]mannitol. The apical washing solution was removed and replaced by 500 μL of a solution with [^{14}C]mannitol (30 μL stock solution in 5 mL HBSS) at the experimental pH conditions. After 60 min, the samples were taken from the apical and basolateral compartments for activity measurements. A diffusion rate of $\leq 0.5\%$/h was taken as an indicator of normal monolayer integrity (**II**).

4.6 *In vivo* experiments (II and V)

All animal experiments were approved by the National Committee for Animal Experimentation in Finland (State Provincial Office of Southern Finland, Hämeenlinna). The ^{18}F-labeled THCPSi particles (**II** and **V**) were administered to male Wistar Han rats, aged 7-10 weeks, in 5% Solutol-1×HBSS (pH 7.4) either by intragastric gavage (**II** and **V**), subcutaneously on the back (**II**) or *i.v.* via the lateral tail vein (**II**). The control animals received ^{18}F-NaF in 5% Solutol-1×HBSS (pH 7.4). The animals were sacrificed at 2, 4 and 6 h, or at 30 min, 1 and 4 h after administration for enteral and parental routes, respectively.

Samples from blood, urine, mesenteric lymph node, liver lung, kidney, spleen, testis, brain, bone, and stomach were collected and measured for radioactivity. For intestinal biodistribution of particle radioactivity, the lower GI tract was excised and samples were taken from the duodenum, jejunum, ileum, cecum, and the ascending, transverse and descending parts of the intestine. The samples were weighed and their radioactivity was measured with a gamma counter. For the animals dosed with intragastric gavage, the lower gastrointestinal tract was imaged with digital autoradiography prior to sampling for radioactivity counting. The excised intestines were arranged on an imaging plate together with ^{18}F standards, photographed for macroanatomical identification of the different intestinal parts and analyzed with imaging software.

5 Results and discussion

5.1 Particle characterization (I-V)

The PSi particles studied in this dissertation differ between them in several physicochemical properties. While the TOPSi particles are hydrophilic due to their oxide terminated bonds at the surface, THCPSi are hydrophobic due to the hydrogen atoms on the surface. Besides surface area, pore diameter and pore volume of both TOPSi and plain THCPSi micro- and nanoparticles, HFBII coated particles were also characterized. The results are presented in Table 5.

Table 5 *Characterization of TOPSi, plain THCPSi and HFBII-coated THCPSi particles.*

Particle	Surface area (m^2/g)	Pore volume (cm^3/g)	Pore diameter (nm)	ζ-potential (mV)
TOPSi micro	202	0.63	9.2	−
TOPSi nano	177	0.63	15.7	-33.7 ± 4.4
THCPSi micro	231	0.63	8.4	−
THCPSi nano	202	0.51	9.0	-34.1 ± 1.9
THCPSi-HFBII micro	180	0.52	8.4	−

The microparticles studied, with size fractions ranging from 1-10 to 25-75 µm, and the nanoparticles, with sizes ranging from 97 to 188 nm, displayed a highly porous structure (Figure 3A), which contributed to their high surface area. The nanoparticles used in the experiments displayed a very uniform spherical shape, with a narrow size distribution (Figure 3B and 3C). The high surface area of the PSi particles enables drug loading and confinement, which in turn increases drug dissolution rates (Salonen *et al.*, 2005). The HFBII coating of the particles carried out in the experiments (**III**) decreased the surface area, which can be partially due to the increase in the sample mass by weight of the HFBII layer. As the pore volume is decreased, it may be possible that a small amount of HFBII may block the pores and thus reducing the available specific surface area and pore volume during the N_2 sorption method.
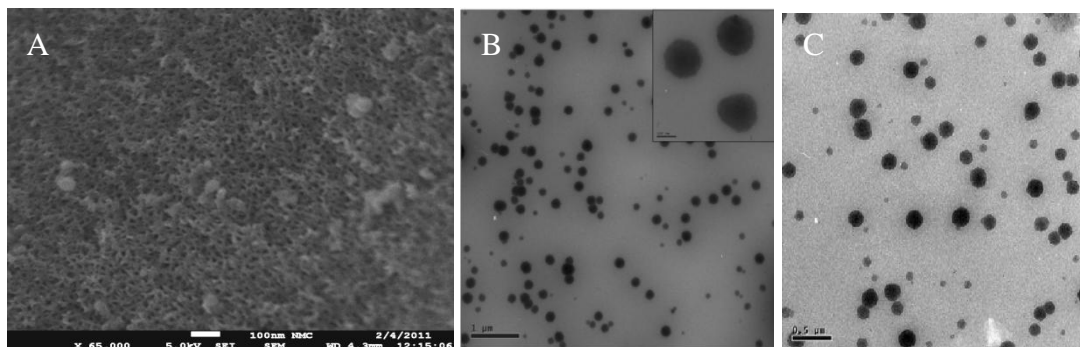
Figure 3 *SEM image of the porosity of PSi particles (A) and TEM images of TOPSi (B) and THCPSi (C) nanoparticles. The scale bars depicted are 100 nm (A), 1 μm and 100 nm for the inset (B) and 0.5 μm (C).Copyright © (2010, 2011) American Chemical Society and Elsevier. Reprinted with permission.*

The pore characteristics of PSi materials can be modulated through the control of generally used diluted HF electrolyte solutions, etching current and surface tension reducing agents. Usually, an increase in current density or anodization potential also leads to an increase in the pore diameter and straighter pores, and the increasing pore sizes generally decrease the interpore connections and pore branching (Zhang, 2001). The decreased surface area and increased average pore diameter of the particles used in our experiments are a result of the different etching current profiles used in the production of the nanoparticles. The current modulates the pore morphology enlarging the pore openings in the nanoparticles, leading to the increase in the average pore diameter and decrease in surface area. Due to the same reason, the pore volume of the nanoparticles remained almost invariable and rather similar to the pore volume of the microparticles (**I**).

The control of the pore properties of PSi is an important parameter when biocompatibility is concerned. The porosity of the PSi based materials has been found to alter their degradation profile, as high-porosity mesoporous films exhibited substantial dissolution, and consequent biodegradability *in vivo* (Canham *et al.*, 1999). Moreover, degradation of PSi particles, is faster under alkaline pH conditions, and it has been found to yield harmless products, such as $Si(OH)_4$ which is excreted in the urine through the kidneys (Jugdaohsingh *et al.*, 2002), and is well tolerated *in vivo* (Park *et al.*, 2009). The PSi porosity degree is also a critical parameter that affects the crystalinization behavior of the drugs inside and outside of the pores as well as the subsequent drug release.

The measured ζ-potential of the studied nanoparticles showed a strongly negatively charged surface, which prevented aggregation and stabilized the particles in suspension. In addition, the HFBII coating maintained the negative charge of the particles (–25.8 ± 13.0), despite adsorbing onto the particles' surface (**V**). The stability of the HFBII coating on the THCPSi particle surface was found to be higher at lower pH values (1.2) and displayed an abrupt decrease on protein desorption from the particles' surface after incubation at pH 7.4 and 37 ℃ (Figure 4). The mechanism of HFBII adsorption to Si surfaces is still poorly understood. However, we have considered that the protein is most likely strongly adsorbed onto the surface of the PSi's surface under the experimental conditions studied. The nature of the hydrophobin protein attraction was hypothesized to be of two types: (1) electrostatic

patch charge attraction, which is due to the presence of an equal number of positively and negatively charged groups arranged in a mosaic pattern at each of the film surfaces, with opposing charge sites facing each other (Richmond, 1974; Basheva *et al.*, 2011); and (2) short–range hydrophobic interaction due to the presence of amino-acid residues with hydrophobic side chains on the water-facing part of the HFBII molecule (Meyer *et al.*, 2006; Hammer *et al.*, 2010). Both these interactions represent a non-covalent binding and, moreover, it has also been reported that the HFBII adsorption to hydrophobic solids was found to be weaker than that of HFBI (Askolin *et al.*, 2006). All together, the strong adsorption of HFBII protein onto the PSi surfaces seems to be the most plausible explanation.
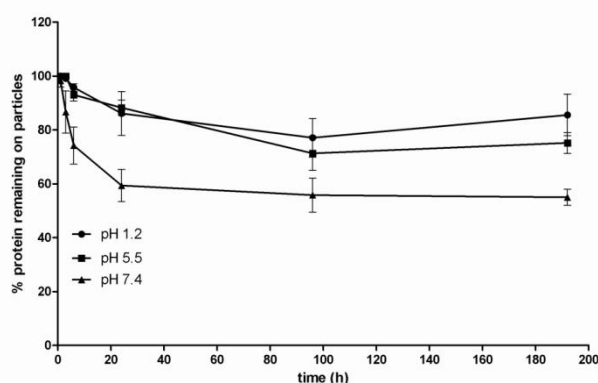
Figure 4   *Stability of the HFBII-coating on the THCPSi particle surface over time at pH values of 1.2, 5.5 and 7.4 after incubation at 37 ºC. Error bars represent SD (n ≥ 3). Copyright © (2011) Elsevier. Reprinted with permission.*

The THCPSi microparticles, when observed under SEM, displayed a pronounced surface roughness, whereas the HFBII coating induced smoothness in the particles' surface (Figure 5).
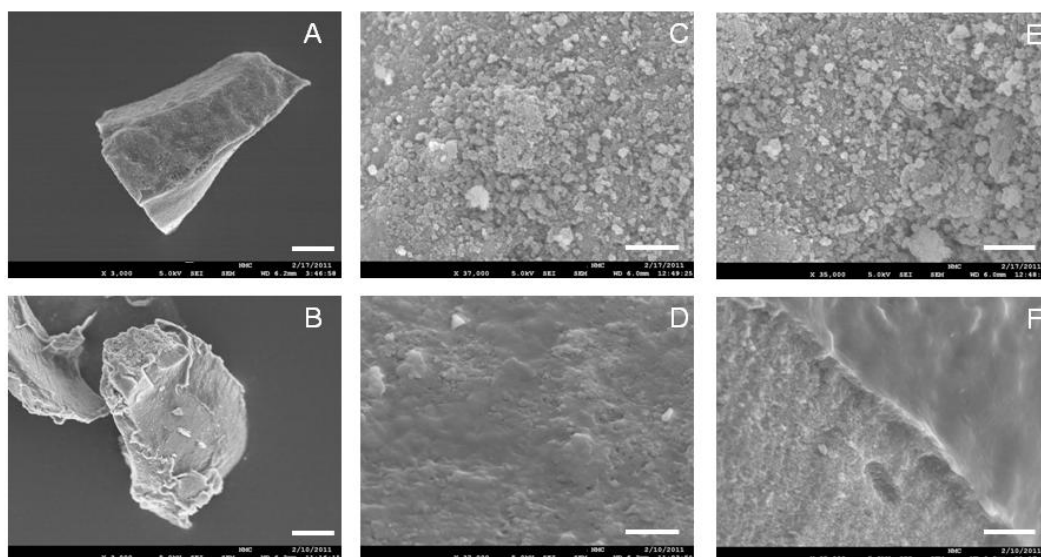

Figure 5   *SEM micrographs of uncoated (A, C and E) and HFBII-coated (B, D and F) THCPSi microparticles. The scale bars depicted are 5 µm (A and B) and 500 nm (C, D, E and F). Copyright © (2011) Elsevier. Reprinted with permission.*

5.2 In vitro biocompatibility assessment (I-V)

Engineered nanostructures have shown great promise in their ability to overcome many of the hurdles for delivering compounds to their desired sites of action. However, there is a great concern about the possible harmful effects that these structures may elicit when they interact with biological systems.

The several tiers of oxidative response elicited by different concentrations, sizes and particle types were studied at different incubation times (**I-V**).The first set of experiments focused on the size and particle type in eliciting the first tier response of oxidative stress, in the form of ROS. The ROS assessment of both TOPSi (**I**) and THCPSi (**II**) showed that no significant increase was obtained in most of the concentrations and sizes studied in both particle types (**I** and **II**). Subsequently, inflammatory response was measured in terms of TNF-α production, which can be regarded as a second tier response of oxidative stress. TNF-α is a polypeptide cytokine produced by macrophages that stimulates acute phase reaction, which means that it can be used as an inflammatory response marker (Choi *et al.*, 2009). Together with NO induction, TNF-α has already been studied as a part of nanoparticle toxicity assessments in RAW 264.7 macrophages (Scheel *et al.*, 2009). However, commercially available enzyme-linked immunosorbent assay (ELISA) for cytokine assessment can lead to differential cytokine binding to micro- and nanoparticles, which might contribute to the underestimation of inflammatory response results (Kocbach *et al.*, 2008). Therefore, after assessing and correcting the values obtained by the ELISA in RAW 264.7 macrophage cells (**I** and **II**), no clear concentration dependence in the cells was observed for the particles studied. Nevertheless, all microparticles, with size fractions of 1-10 and 10-25 µm, triggered a more pronounced inflammatory reaction than most of the nanoparticles, with the exception of the THCPSi particle sizes of 97 nm (**II**).

Although still frequently used in viability determinations of Si particles, it has been shown that the PSi particles react with common colorimetric viability assays such as the MTT (Laaksonen *et al.*, 2007) or LDH, which leads to overestimation of the cellular viability. Other reports have also suggested some limitations of most common cellular viability assays when nanomaterials are concerned (Monteiro-Riviere *et al.*, 2009). To investigate the toxic response of the PSi materials, the particles were incubated with several cell lines for 6, 12 or 24 h and cell viability was assessed by two different methods: (1) a luminescent method (**I-V**) based on the quantification of the metabolically active (in terms of ATP content) cells (AshaRani *et al.*, 2009; Santos *et al.*, 2010); and (2) a fluorescent method (**I**) based on the detection of a conserved and constitutive protease activity associated with intact viable cells. The plain PSi micro- and nanoparticles.and their HFBII-coated counterparts were also evaluated in terms of their cytotoxicity at different concentrations. All uncoated particle types showed a size and concentration-dependent toxicity, with microparticles particles eliciting the greatest cytotoxic response (Figure 6).
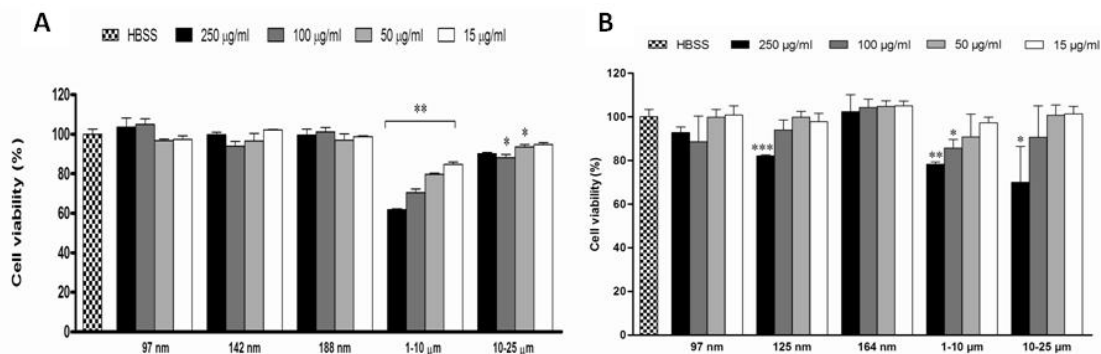
Figure 6 *Cell viability of Caco-2 cells incubated with THCPSi (A) and TOPSi (B) particles at 24 h assessed by a luminescence-based assay. Error bars represent SD (n ≥ 3). Statistical analysis was made by ANOVA followed by a Dunnet's multiple comparison test. All data sets were compared with a negative cytotoxicity control of HBSS.The level of significance was set at probability of *p < 0.05, **p < 0.01 and ***p < 0.001. Copyright © (2010, 2011) American Chemical Society and Elsevier. Reprinted with permission.*

The HFBII coating also changed the hydrophilicity of the THCPSi surfaces, turning them from hydrophobic to hydrophilic (**III-V**). This subsequent shift in hydrophobicity improved the particles' biocompatibility, as already reported for other types of surfaces (Hezi-Yamit *et al.*, 2009).The HFBII coating significantly increased the cell viability compared to uncoated particles both in micro- and nanoparticles (Figure 7). Microparticles were found to elicit the greatest cytotoxic response and the HFBII coating significantly improved the cell viability at concentrations of 50 and 15 µg/mL (Figure 7A), whereas in the case of nanoparticles the improvement in viability was significant at concentrations of 500 and 250 µg/mL (Figure 7B)
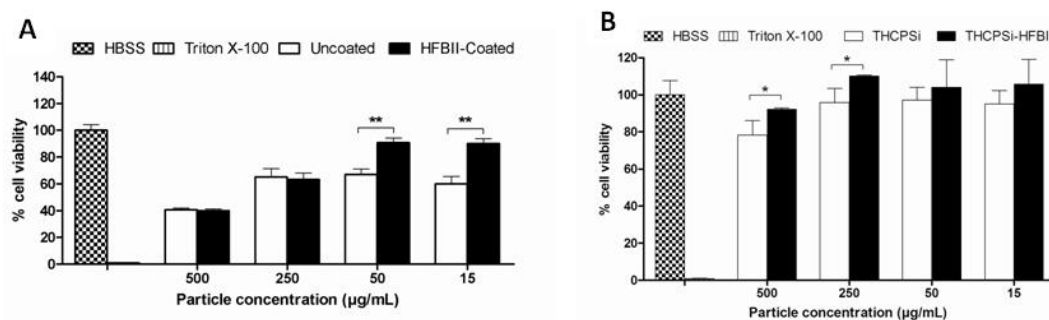
Figure 7 *Cell viability of Caco-2 cells incubated with HFBII-coated THCPSi micro- (A) and nanoparticles (B) assessed by a luminescence-based assay. Error bars represent SD (n ≥ 3). Statistical analysis was made by the Student's t-test. The cell viability of uncoated particles was compared with their coated counterparts. The level of significance was set at probability of p < 0.05 for *, p < 0.01 for **. Copyright © (2011) Elsevier (2011). Reprinted with permission.*

5.3 Drug release experiments (III)

Drug release studies were made in order to evaluate the efficacy of the drug loading and the effect of the HFBII-coating on the drug release from PSi. At pH 1.2 it was observed that the uncoated THCPSi particles released ~12% of the loaded IMC after 120 min, but the HFBII-coated particles did not release any drug in the same time interval (Figure 8A). However, at pH 5.5 the drug release profiles were similar, with both types of particles releasing more than 90% of the loaded IMC at 48 h (Figure 8B). At pH 7.4, the IMC release rate was even faster, with more than 90% of drug released after 90 min for both the uncoated and the coated particles (Figure 8C).
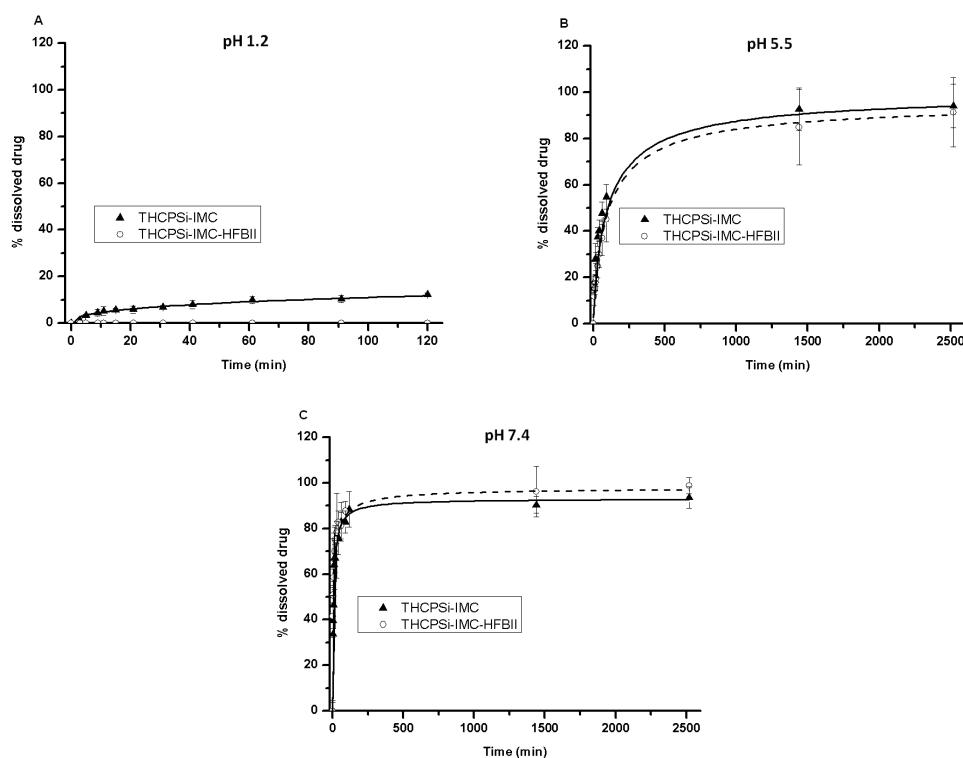

Figure 8   *Drug release profiles of IMC-loaded THCPSi (▲) and IMC-loaded HFBII-coated THCPSi (○) microparticles in buffer solutions at pH values of 1.2 (A), 5.5 (B) and 7.4 (C) at 37 °C. Dissolution medium was 0.2 M HCl/KCl (pH 1.2), 10 mM MES (pH 5.5) and 10 mM HEPES (pH 7.4). Error bars represent ±SD (n ≥ 3). Copyright © (2011) Elsevier. Reprinted with permission.*

Although both the uncoated and coated THCPSi particles allowed a fast IMC release, only the coated particles seem to protect the drug release at low pH-values, which makes the HFBII-coated THCPSi particles a promising pH-responsive carrier for oral drug delivery. As the pH is increased, a gradually faster IMC release is observed, which is rather advantageous due to the differences in the pH conditions along the GI tract. These results show that despite the HFBII-coating, which rendered the particles hydrophilic, there was no significant hindering of the IMC release at pH values of 5.5 and 7.4 (similarly to the uncoated THCPSi particles). However, at pH 1.2 there was no IMC release from the pores of the HFBII-coated particles unlike the uncoated ones. This feature is significant for the

protection of the drug against the harsh conditions of the stomach, avoiding possible degradation of the drug and even precipitation, which may hinder an efficient absorption of the drug in the intestine and reducing the drug's pharmacological activity.

5.4 Compound permeation (I-V)

Caco-2 are human colon epithelial cancer cells that have been widely used as a model of human intestinal absorption of drugs and other compounds (Yee, 1997; van Breemen and Li, 2005). The permeation of compounds across the Caco-2 cell monolayer has also been shown to correlate with the fractional oral absorption data in humans (Artursson and Karlsson, 1991). In addition, Caco-2 cells express transporter proteins, efflux proteins, and Phase II conjugation enzymes to model a variety of transcellular pathways as well as metabolic transformation of test substances (van Breemen and Li, 2005). To validate the efficacy of the TOPSi nanoparticulate delivery system, the permeation properties of the nanoparticles loaded with griseofulvin (an antifungal drug) with a size of approximately 170 nm were assessed (**I**). The results show a significant increase in drug permeation across the Caco-2 monolayers compared with the bulk drug at both pH 5.5 and 7.4 (Figure 9A and 9B). This is probably due to the enhanced drug solubility obtained as a result of its loading into the TOPSi nanoparticles and consequent attainment of high local concentrations, and even drug supersaturation, which can increase the net drug absorption and respective permeation (Kaukonen *et al.*, 2007; Brouwers *et al.*, 2009).
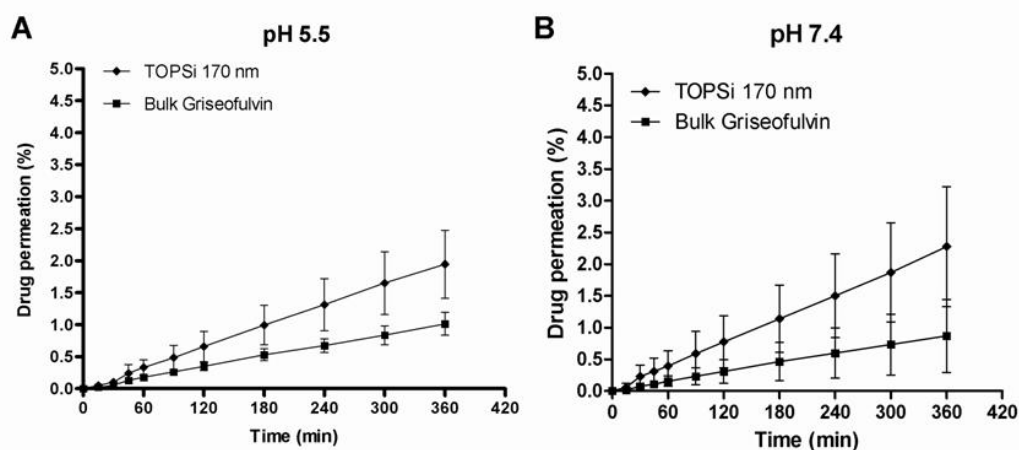
Figure 9 *Permeation of bulk griseofulvin (■) and griseofulvin loaded TOPSi nanoparticles of 170 nm (♦) across a differentiated Caco-2 cell monolayer at apical pH of 5.5 (A) and 7.4 (B). The basolateral solution was kept at pH 7.4 in all experiments. Error bars represent SD (n≥3). Copyright © (2011) Elsevier. Reprinted with permission.*

As HFBII is a protein known to be extremely surface active, the question whether the HFBII-coating of the micro- and nanoparticles interfered with the drug permeation was raised. The permeation of IMC across a differentiated Caco-2 cell monolayer from the loaded THCPSi microparticles showed a significant increase when compared with bulk

IMC at pH values of 5.5 (Figure 10A) and 7.4 (Figure 10B). About 7% of the IMC permeated across the Caco-2 monolayer after 240 min when loaded into the THCPSi microparticles, whereas only 2% of the bulk IMC permeated in the same time interval at pH 5.5 (Figure 10A). At pH 7.4, the coated and uncoated IMC-loaded THCPSi microparticles showed no significant differences in the permeation profiles, with about 30% of IMC permeating across the Caco-2 monolayer after 240 min (Figure 10B). The bulk IMC however, only permeated 20% across the cell monolayer (Figure 10B). These results suggest that the coated microparticles did not disrupt in any way the cell monolayer, nor hampered the permeation of IMC from the THCPSi particles (Figure 10A and 10B). The increase in the IMC permeation observed is probably due to the enhanced solubility of the drug as a result of the loading into the THCPSi microparticles (**III**). For the HFBII-coated THCPSi nanoparticles, the results showed that the IMC permeation rate from the particles was found not to be significantly different from an IMC solution (Figure 10C). The IMC amount permeated across the differentiated Caco-2 monolayer was around 22% for the HFBII-coated THCPSi and IMC solution after 240 min.
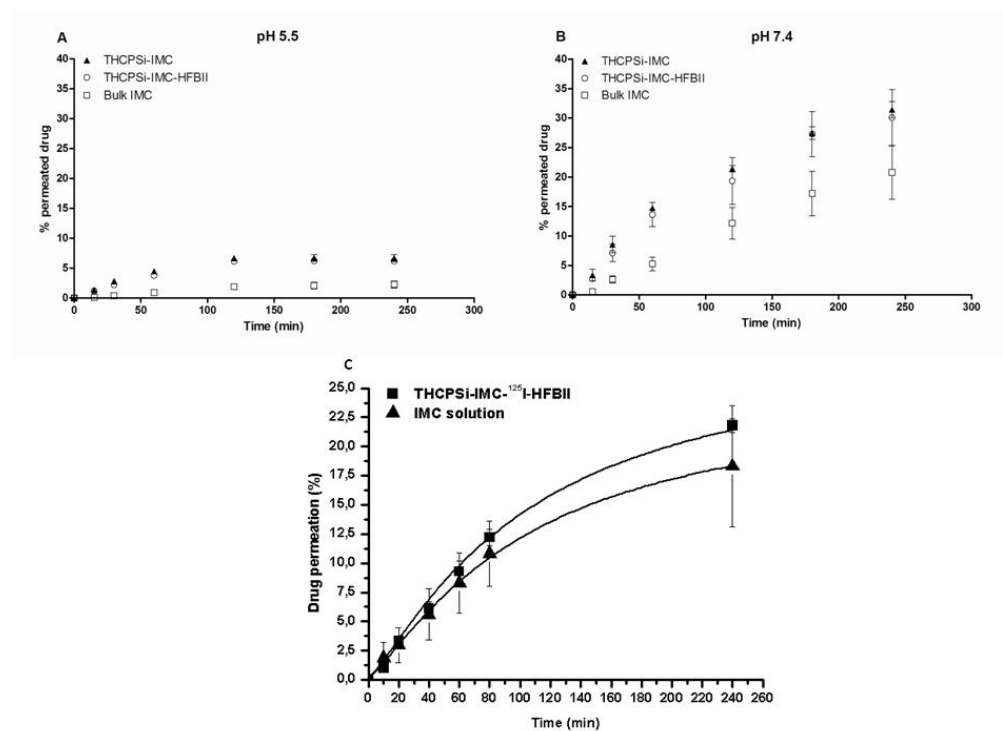

Figure 10 *Permeation of bulk IMC (□), IMC solution (△), THCPSi-IMC, (▲), THCPSi-IMC-HFBII (○) and THCPSi-IMC-^{125}I-HFBII (■) nanoparticles across a differentiated Caco-2 cell monolayer at apical pH of 5.5 (A) and 7.4 (B and C). The basolateral solution was kept at pH 7.4 in all experiments. Error bars represent SD (n≥3). Copyright © (2011) Elsevier. Reprinted with permission.*

The increase in permeation from the TOPSi and THCPSi particles suggests that PSi can increase the solubility and, consequently, the drug permeation of poorly water-soluble drugs, regardless of particles' surface chemistry. The HFBII coating on both THCPSi micro- and nanoparticles was also found not to hamper in any way the drug release or to disturb the Caco-2 cell monolayer.

5.5 Cellular interaction (I-IV)

TOPSi microparticles, despite being in contact with the polarized Caco-2 cell monolayer for 24 h, did not attach or were internalized into the monolayer (Figure 11A and 11B). However, they seemed to remain in the close vicinity of the microvilli, which can be regarded as an advantageous property, as they can function as drug depots at the cell surface. This is the first reported evidence of such phenomenon. The TOPSi microparticles (1–10 µm) in contact with the RAW 264.7 macrophages were readily phagocytized at 50 µg/mL (Figure 11C), which lead in some cases to the disruption of the nuclear membrane. The particles seemed to be sequestered inside the lysosomal compartment for the duration of the assay, without any evidence of degradation (Figure 11D).
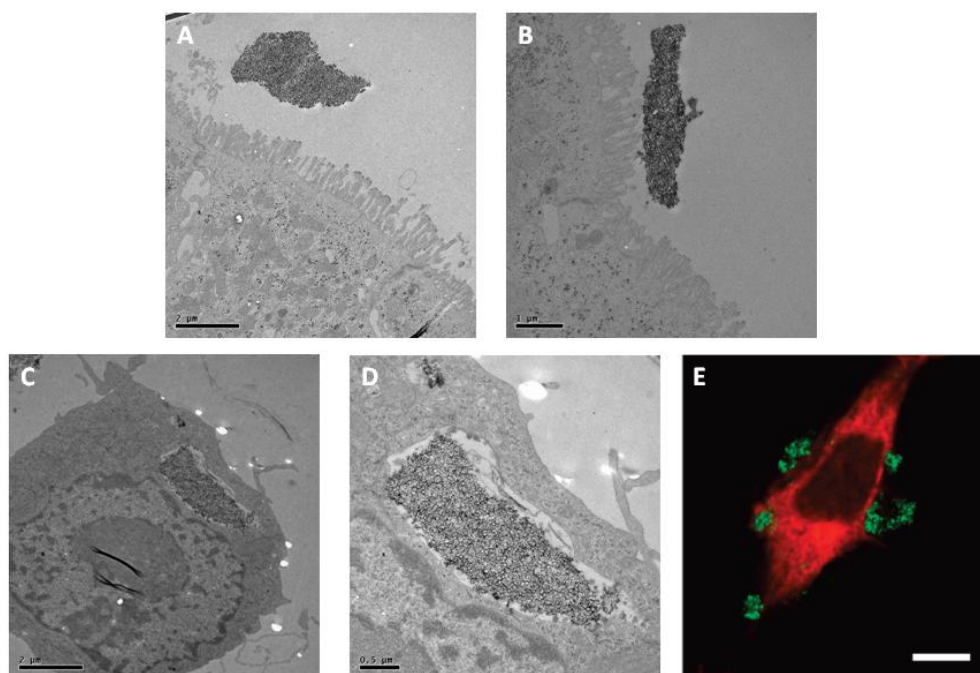

Figure 11 *TEM pictures (A, B, C and D) of flat embedded ultrathin sections of TOPSi microparticles (1-10 µm, 50 µg/mL) interactions with Caco-2 (A and B) and RAW 264.7 macrophages(C and D) (scale bars are 2 µm for A and C, 1 µm for B and 500 nm for D). Confocal microscopy images (E) of a RAW 264.7 macrophage stained in orang, interacting with FITC-THCPSi nanoparticles labeled green (scale bar 5 µm). Copyright © (2010, 2011) American Chemical Society and Elsevier. Reprinted with permission.*

It was also observed that the majority of the THCPSi nanoparticles remained attached to the cell surface (Figure 11E). Positively charged particles were found to be internalized in a much greater extent than negatively charged particles (Gratton *et al.*, 2008). Therefore, we postulate that the negative ζ-potential of THCPSi particles together with their hydrophobic nature favors a strong particle-membrane interaction (Tavares *et al.*, 2009), but extensive internalization is prevented (Gratton *et al.*, 2008). The strong membrane interaction due to the THCPSi hydrophobic nature could cause toxicity (Tavares *et al.*, 2009), an effect attenuated with the HFBII coating of these particles (**III-V**). Nonetheless, the HFBII-coating of the PSi, despite maintaining the negative surface charge, was found to modulate

the adsorption of different types of proteins to the particles (Sarparanta *et al.*, 2011), leading to a change in the composition of the corona (Walczyk *et al.*, 2010), which in turn is implied in modulating cellular responses and biocompatibility (Kunzler *et al.*, 2007; Myllymaa *et al.*, 2010). Another important feature of the HFBII proteins is their ability to prevent other protein's adhesion onto coated surfaces (Wang *et al.*, 2010), which could be further explored for increased biocompatibility and particle *i.v.* applications.

5.6 Biodistribution in rats (II and V)

The suitability of THCPSi nanocarriers for drug delivery applications needs to be validated by biodistribution studies *in vivo* in order to establish a proof of principle for human applications. The FITC-label is quenched in acidic environments such as the stomach and is, therefore, unsuitable for labeling particles intended for oral administration. Instead, radiolabeled ^{18}F-THCPSi nanoparticles were administered to male Wistar rats using three different routes: oral administration by intragastric gavage, subcutaneous and intravenous injections. The [^{18}F]fluoride ion is a known bone-seeking radiotracer, showing high and rapid bone uptake in rats (Charkes *et al.*, 1979; Schou *et al.*, 2004). The control animals received ^{18}F-NaF in the vehicle to establish the biodistribution pattern of free [^{18}F]fluoride. The ^{18}F accumulation in bone is commonly regarded as an indicator of the level of defluorination of the tracer *in vivo* (Charkes *et al.*, 1979). Therefore, the administration to control animals of [^{18}F]F[-] as sodium fluoride to differentiate the biodistribution of ^{18}F-labeled nanoparticles from detached free ^{18}F label was a crucial point to address. The results showed that the nanoparticles did not cross the intestinal wall, as seen by the negligible amount of radioactivity detected in the systemic circulation or organs outside the GI tract (Figure 12 A and 12B).
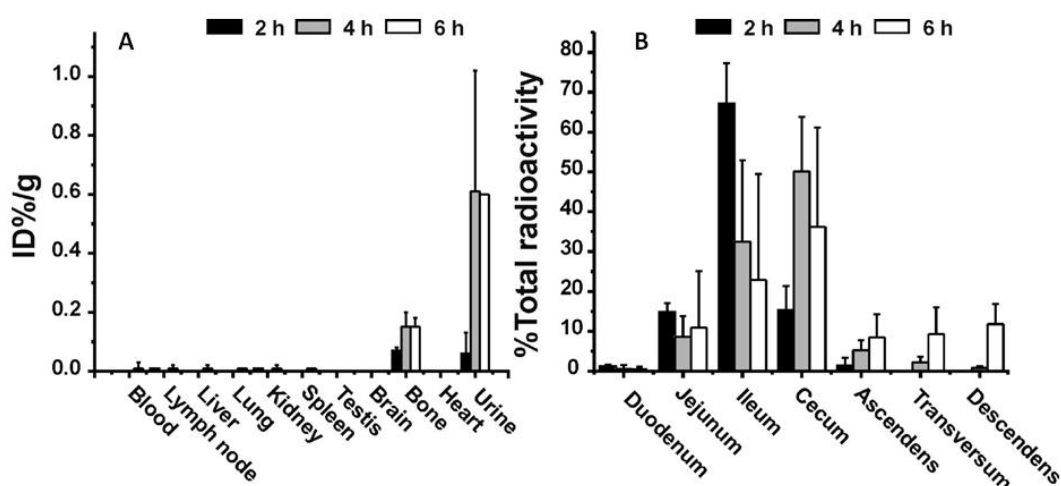

Figure 12 *Biodistribution of ^{18}F-labeled THCPSi nanoparticles after oral administration (A) and their radioactivity distribution in the lower GI tract (B), as quantified by autoradiography (n= 3–4 at each time point; mean ± SD). Copyright © (2010) American Chemical Society. Reprinted with permission.*

The observed appearance of radioactivity in bone and urine (< 0.6 ID%/g) at later time points was speculated to be due to minor detachment of the ^{18}F-label, which can be caused by the *in vivo* defluorination or disintegration of the particles themselves. After *i.v.* administration into the lateral tail vein, the particles were found in the liver and spleen indicating that they are rapidly removed from the circulation. The THCPSi nanoparticles that were administered subcutaneously under the loose skin at the back of the animal resided in the subcutaneous space for up to 4 h post injection. The biodistribution data for subcutaneous administration showed only minimal leakage of dissociated ^{18}F-label into the circulation and subsequent accumulation in bone and urine. As expected, significantly higher ^{18}F bone uptake was seen in control animals in all administration routes. In addition, free ^{18}F was rapidly extracted into urine in large amounts after *i.v.* and subcutaneous injections, whereas in particle-dosed animals less than 1 ID%/g was excreted via the kidneys (Figure 12A). In control animals dosed orally, slightly slower kinetics of bone uptake were observed compared to the parenteral routes.

The HFBII coating was also found to endow the THCPSi nanoparticles of gastroretentive properties. Upon entry of THCPSi-^{18}F-HFBII nanoparticles from the stomach into the intestines, it was observed that the particles were experiencing a delay compared with the uncoated ones. The HFBII-coated nanoparticles were found to be retained in the stomach up to three hours after administration, whereas the uncoated THCPSi were released in two hours in the same conditions (Figure 13). Interestingly, the amount of THCPSi-^{18}F-HFBII nanoparticles retained in the stomach seems to peak at 2-3 hours after administration, suggesting that the nanoparticles are not immediately attached to the gastric mucosa, and are leached out as loose particles when the stomach is emptied.
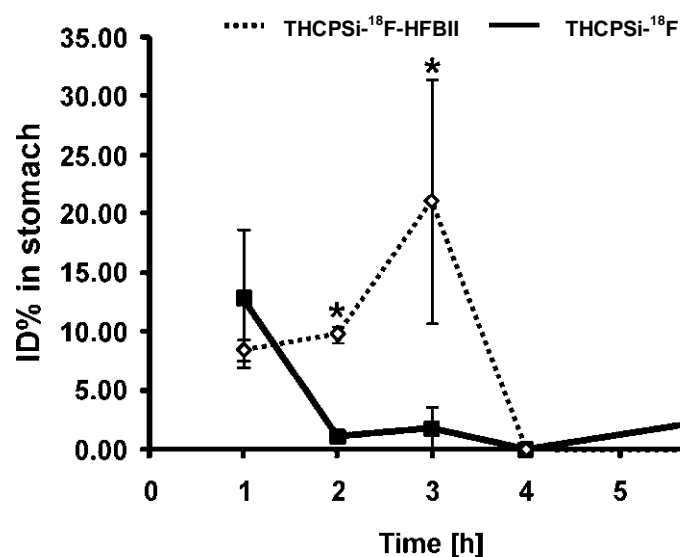
Figure 13 *Gastric clearance of THCPSi-^{18}F-HFBII nanoparticles versus uncoated THCPSi-[18]Fnanoparticles. Values denote mean ± SD (n = 3). The level of significance was set at probability of p < 0.05 for *.*

6 Conclusions and future perspectives

The studies in this thesis ascertain the biocompatibility of PSi materials, regarding their inflammatory response, oxidative aggression and cell toxicity. The studies highlight different surface treated PSi micro- and nanoparticles and their ability to improve drug dissolution and drug permeation across biological barriers. By increasing the particle dissolution it is possible to achieve a higher drug concentration at the target site, therefore increasing the chances of a successful therapeutic outcome. Furthermore, the concentration and size dependent toxicity of these particulate systems was systematically established. Significant differences were found regarding several biocompatibility parameters between micro- and nanoparticles, which can impact the biomedical applications of these systems. PSi microparticles were shown to be more toxic than their nanoparticle counterparts. The nanoparticles were also found not to permeate across the gastrointestinal wall, but allowed the loaded drug to be released and become freely available for absorption. Once the particles were dissolved, they yielded harmless degradation products in the form of silicic acid. The relevance of this kind of technology is many folds, especially in solid state pharmaceutical and nanomedicine applications. The biodistribution of thermally hydrocarbonized PSi nanoparticles was also examined, showing that the intravenously injected nanoparticles were quickly sequestered to the liver and spleen. The employment of a self-assembling protein to coat the particles was also object of investigation. The coating was found to reverse the hydrophobicity and improved the biocompatibility of hydrophobic particles with several cell lines. The hydrophobin class II coating onto the particles was also found not to disturb the drug release from the pores of the particles and to improve cell association. The increased cell association is hypothesized to allow the release of the drug in closer vicinity to the cells, and therefore, increasing the drug's bioavailability. These coated nanoparticles were also found to possess gastro-retentive properties, allowing them to be employed with drugs with a narrow window of absorption. The gastro-retentive properties and the particle's coating stability were validated both *in vitro* and *in vivo* using radiolabeled particles. The results showed that the coating was stable for several hours and that the particles lost their coating and gastro-retention after being retained in the stomach for more than three hours. PSi particles emerge hence as a very promising platform for controlled drug delivery and imaging applications.

Further functionalization, endowing the particles with shielding for opsonization and active targeting, is envisioned in the future. Multiple cargo loading, with small molecule drugs and DNA material for genetic therapy are also conjectured, allowing the PSi nanoparticles to fulfill their role as promising nanomedicine carriers.

References

Ahmed, A., Bonner, C. and Desai, T.A. 2002. Bioadhesive microdevices with multiple reservoirs: a new platform for oral drug delivery. J. Control. Release 81(3): 291-306.

Aimanianda, V., Bayry, J., Bozza, S., Kniemeyer, O., Perruccio, K., Elluru, S.R., Clavaud, C., Paris, S., Brakhage, A.A., Kaveri, S.V., Romani, L. and Latge, J.P. 2009. Surface hydrophobin prevents immune recognition of airborne fungal spores. Nature 460(7259): 1117-1121.

Ainslie, K.M., Tao, S.L., Popat, K.C. and Desai, T.A. 2008. In vitro Immunogenicity of Silicon-Based Micro- and Nanostructured Surfaces. ACS Nano 2(5): 1076-1084.

Akanbi, M.H.J., Post, E., Meter-Arkema, A., Rink, R., Robillard, G.T., Wang, X.Q., Wosten, H.A.B. and Scholtmeijer, K. 2010. Use of hydrophobins in formulation of water insoluble drugs for oral administration. Colloids Surf. B 75(2): 526-531.

Alvarez, S.D., Derfus, A.M., Schwartz, M.P., Bhatia, S.N. and Sailor, M.J. 2009. The compatibility of hepatocytes with chemically modified porous silicon with reference to in vitro biosensors. Biomaterials 30(1): 26-34.

Ameyar, M., Wisniewska, M. and Weitzman, J.B. 2003. A role for AP-1 in apoptosis: the case for and against. Biochimie 85(8): 747-752

Anderson, S.H.C., Elliott, H., Wallis, D.J., Canham, L.T. and Powell, J.J. 2003. Dissolution of different forms of partially porous silicon wafers under simulated physiological conditions. Phys. Status Solidi A 197(2): 331-335.

Anglin, E.J., Cheng, L., Freeman, W.R. and Sailor, M.J. 2008. Porous silicon in drug delivery devices and materials. Adv. Drug Deliv. Rev. 60(11): 1266-1277.

Anglin, E.J., Schwartz, M.P., Ng, V.P., Perelman, L.A. and Sailor, M.J. 2004. Engineering the Chemistry and Nanostructure of Porous Silicon Fabry-Pérot Films for Loading and Release of a Steroid. Langmuir 20(25): 11264-11269.

Archer, R.J. 1960. Stain films on silicon. J. Phys. Chem. Solids 14: 104-110.

Arroyo-Hernández, M., Martı, amp, x, n-Palma, R.J., Pérez-Rigueiro, J., Garcı, a-Ruiz, J.P., a-Fierro, J.L. and nez-Duart, J.M. 2003. Biofunctionalization of surfaces of nanostructured porous silicon. Mater. Sci. Eng. 23(6-8): 697-701.

Arroyo-Hernandez, M., Perez-Rigueiro, J. and Martinez-Duart, J.M. 2006. Formation of amine functionalized films by chemical vapour deposition. Mater. Sci. Eng. C 26(5-7): 938-941.

Artursson, P. and Karlsson, J. 1991. Correlation between oral drug absorption in humans and apparent drug permeability coefficients in human intestinal epithelial (Caco-2) cells. Biochem. Biophys. Res. Commun. 175(3): 880-885.

AshaRani, P.V., Low Kah Mun, G., Hande, M.P. and Valiyaveettil, S. 2009. Cytotoxicity and genotoxicity of silver nanoparticles in human cells. ACS Nano 3(2): 279-290.

Askolin, S., Linder, M., Scholtmeijer, K., Tenkanen, M., Penttila, M., de Vocht, M.L. and Wosten, H.A. 2006. Interaction and comparison of a class I hydrophobin from Schizophyllum commune and class II hydrophobins from Trichoderma reesei. Biomacromolecules 7(4): 1295-1301.

Avdeef, A. 2001. Physicochemical profiling (solubility, permeability and charge state). Curr. Top. Med. Chem. 1(4): 277-351.

Basheva, E.S., Kralchevsky, P.A., Danov, K.D., Stoyanov, S.D., Blijdenstein, T.B., Pelan, E.G. and Lips, A. 2011. Self-assembled bilayers from the protein HFBII hydrophobin: nature of the adhesion energy. Langmuir 27(8): 4481-4488.

Bayliss, S.C., Buckberry, L.D., Harris, P.J. and Tobin, M. 2000. Nature of the Silicon-Animal Cell Interface. J. Porous Mater. 7(1): 191-195.

Bayliss, S.C., Heald, R., Fletcher, D.I. and Buckberry, L.D. 1999. The Culture of Mammalian Cells on Nanostructured Silicon. Adv. Mater. 11(4): 318-321.

41

Beckmann, K.H. 1965. Investigation of the chemical properties of stain films on silicon by means of infrared spectroscopy. Surf. Sci. 3(4): 314-332.

Björkqvist, M., Salonen, J., Paski, J. and Laine, E. 2004. Characterization of thermally carbonized porous silicon humidity sensor. Sens. Actuators, A 112(2-3): 244-247.

Bolton, A.E. and Hunter, W.M. 1973. The labelling of proteins to high specific radioactivities by conjugation to a 125I-containing acylating agent. Biochem. J. 133(3): 529-539.

Bonanno, L.M. and Delouise, L.A. 2010. Tunable detection sensitivity of opiates in urine via a label-free porous silicon competitive inhibition immunosensor. Anal. Chem. 82(2): 714-722.

Boukherroub, R., Wojtyk, J.T.C., Wayner, D.D.M. and Lockwood, D.J. 2002. Thermal hydrosilylation of undecylenic acid with porous silicon. J. Electrochem. Soc. 149(2): H59-H63.

Bowditch, A.P., Waters, K., Gale, H., Rice, P., Scott, E.A.M., Canham, L.T., Reeves, C.L., Loni, A. and Cox, T.I. 1999. In-vivo assessment of tissue compatibility and calcification of bulk and porous silicon. Mater. Res. Soc. Symp. P 536: 149-154.

Braeckmans, K., De Smedt, S.C., Leblans, M., Pauwels, R. and Demeester, J. 2002. Encoding microcarriers: present and future technologies. Nat. Rev. Drug Discov. 1(6): 447-456.

Brigger, I., Dubernet, C. and Couvreur, P. 2002. Nanoparticles in cancer therapy and diagnosis. Adv. Drug Deliv. Rev. 54(5): 631-651.

Brouwers, J., Brewster, M.E. and Augustijns, P. 2009. Supersaturating drug delivery systems: the answer to solubility-limited oral bioavailability? J. Pharm. Sci. 98(8): 2549-2572.

Buriak, J.M. 1999. Silicon-carbon bonds on porous silicon surfaces. Adv. Mater. 11(3): 265-267.

Buriak, J.M. and Allen, M.J. 1998. Lewis Acid Mediated Functionalization of Porous Silicon with Substituted Alkenes and Alkynes. J. Am. Chem. Soc. 120(6): 1339-1340.

Buriak, J.M. and Stewart, M.P. 1998. Photopatterned hydrosilylation on porous silicon. Angew. Chem. Int. Ed. 37(23): 3257-3260.

Burrows, V.A., Chabal, Y.J., Higashi, G.S., Raghavachari, K. and Christman, S.B. 1988. Infrared spectroscopy of Si(111) surfaces after HF treatment: Hydrogen termination and surface morphology. Appl. Phys. Lett. 53(11): 998-1000.

Canham, L.T. 1990. Silicon quantum wire array fabrication by electrochemical and chemical dissolution of wafers. Appl. Phys. Lett. 57(10): 1046-1048.

Canham, L.T., Houlton, M.R., Leong, W.Y., Pickering, C. and Keen, J.M. 1991. Atmospheric impregnation of porous silicon at room temperature. J. Appl. Phys. 70(1): 422-431.

Canham, L.T. 1995. Bioactive silicon structure fabrication through nanoetching techniques. Adv. Mater. 7(12): 1033-1037.

Canham, L.T., Cox, T.I., Loni, A. and Simons, A.J. 1996. Progress towards silicon optoelectronics using porous silicon technology. Appl. Surf. Sci. 102(0): 436-441.

Canham, L.T., Newey, J.P., Reeves, C.L., Houlton, M.R., Loni, A., Simons, A.J. and Cox, T.I. 1996. The effects of DC electric currents on the in-vitro calcification of bioactive silicon wafers. Adv. Mater. 8(10): 847-849.

Canham, L.T. and Reeves, C.L. 1996. Apatite nucleation on low porosity silicon in acellular simulated body fluids. Mater. Res. Soc. Symp. P 414: 189-194.

Canham, L.T., Reeves, C.L., King, D.O., Branfield, P.J., Crabb, J.G. and Ward, M.C.L. 1996. Bioactive polycrystalline silicon. Adv. Mater. 8(10): 850-852.

Canham, L.T. 1997. Properties of porous silicon. Institution of Engineering and Technology. London.

Canham, L.T., Reeves, C.L., Newey, J.P., Houlton, M.R., Cox, T.I., Buriak, J.M. and Stewart, M.P. 1999. Derivatized mesoporous silicon with dramatically improved stability in simulated human blood plasma. Adv. Mater. 11(18): 1505-1507.

Canham, L. 2000. Porous silicon as a therapeutic biomaterial. 1st Annual International Ieee-Embs Special Topic Conference on Microtechnologies in Medicine & Biology, Proceedings: 109-112.

Chan, P.L. and Holford, N.H. 2001. Drug treatment effects on disease progression. Annu. Rev. Pharmacol. 41: 625-659.

Charkes, N.D., Brookes, M. and Makler, P.T. 1979. Studies of Skeletal Tracer Kinetics .2. Evaluation of a 5-Compartment Model of [Fluoride-F-18 Kinetics in Rats. J. Nucl. Med. 20(11): 1150-1157.

Cheng, L., Anglin, E., Cunin, F., Kim, D., Sailor, M.J., Falkenstein, I., Tammewar, A. and Freeman, W.R. 2008. Intravitreal properties of porous silicon photonic crystals: A potential self-reporting intraocular drugdelivery vehicle. Brit. J. Ophthalmol. 92(5): 705-711.

Chiappini, C., Tasciotti, E., Fakhoury, J.R., Fine, D., Pullan, L., Wang, Y.-C., Fu, L., Liu, X. and Ferrari, M. 2010. Tailored porous silicon microparticles: fabrication and properties. ChemPhysChem 11(5): 1029-1035.

Chin, V., Collins, B.E., Sailor, M.J. and Bhatia, S.N. 2001. Compatibility of primary hepatocytes with oxidized nanoporous silicon. Adv. Mater. 13(24): 1877-1880.

Choi, J., Zhang, Q., Reipa, V., Wang, N.S., Stratmeyer, M.E., Hitchins, V.M. and Goering, P.L. 2009. Comparison of cytotoxic and inflammatory responses of photoluminescent silicon nanoparticles with silicon micron-sized particles in RAW 264.7 macrophages. J. Appl. Toxicol. 29(1): 52-60.

Chopra, N., Gavalas, V.G., Bachas, L.G. and Hinds, B.J. 2007. Functional one-dimensional nanomaterials: applications in nanoscale biosensors. Anal. Lett. 40(11): 2067-2096.

Chu, W.H., Chin, R., Huen, T. and Ferrari, M. 1999. Silicon membrane nanofilters from sacrificial oxide removal. J. Microelectromech. S. 8(1): 34-42.

Coffer, J.L., Montchamp, J.-L., Aimone, J.B. and Weis, R.P. 2003. Routes to calcified porous silicon: implications for drug delivery and biosensing. Phys. Status Solidi A 197(2): 336-339.

Collins, B.E., Dancil, K.P.S., Abbi, G. and Sailor, M.J. 2002. Determining protein size using an electrochemically machined pore gradient in silicon. Adv. Funct. Mater. 12(3): 187-191.

Couvreur, P. and Vauthier, C. 2006. Nanotechnology: intelligent design to treat complex disease. Pharm. Res. 23(7): 1417-1450.

Cullis, A.G., Canham, L.T. and Calcott, P.D.J. 1997. The structural and luminescence properties of porous silicon. J. Appl. Phys. 82(3): 909-965.

De Angelis, F., Pujia, A., Falcone, C., Iaccino, E., Palmieri, C., Liberale, C., Mecarini, F., Candeloro, P., Luberto, L., de Laurentiis, A., Das, G., Scala, G. and Di Fabrizio, E. 2010. Water soluble nanoporous nanoparticle for in vivo targeted drug delivery and controlled release in B cells tumor context. Nanoscale 2(10): 2230-2236.

De Jong, W.H. and Borm, P.J. 2008. Drug delivery and nanoparticles:applications and hazards. Int. J. Nanomed. 3(2): 133-149.

De Stefano, L., Rea, I., Armenante, A., Giardina, P., Giocondo, M. and Rendina, I. 2007. Self-assembled biofilm of hydrophobins protects the silicon surface in the KOH wet etch process. Langmuir 23(15): 7920-7922.

De Stefano, L., Rea, I., De Tommasi, E., Rendina, I., Rotiroti, L., Giocondo, M., Longobardi, S., Armenante, A. and Giardina, P. 2009. Bioactive modification of silicon surface using self-assembled hydrophobins from Pleurotus ostreatus. Eur. Phys. J. E 30(2): 181-185.

De Stefano, L., Rea, I., Giardina, P., Armenante, A. and Rendina, I. 2008. Protein-modified porous silicon nanostructures. Adv. Mater. 20(8): 1529-1533.

Decuzzi, P., Lee, S., Decuzzi, M. and Ferrari, M. 2004. Adhesion of microfabricated particles on vascular endothelium: A parametric analysis. Ann. Biomed. Eng. 32(6): 793-802.

Decuzzi, P., Lee, S., Bhushan, B. and Ferrari, M. 2005. A theoretical model for the margination of particles within blood vessels. Ann. Biomed. Eng. 33(2): 179-190.

Decuzzi, P. and Ferrari, M. 2008. Design maps for nanoparticles targeting the diseased microvasculature. Biomaterials 29(3): 377-384.

Decuzzi, P., Pasqualini, R., Arap, W. and Ferrari, M. 2009. Intravascular delivery of particulate systems: does geometry really matter? Pharm. Res. 26(1): 235-243.

Decuzzi, P., Godin, B., Tanaka, T., Lee, S.Y., Chiappini, C., Liu, X. and Ferrari, M. 2010. Size and shape effects in the biodistribution of intravascularly injected particles. J. Control. Release 141(3): 320-327.

Desai, T.A., Hansford, D.J., Kulinsky, L., Nashat, A.H., Rasi, G., Tu, J., Wang, Y., Zhang, M. and Ferrari, M. 1999. Nanopore technology for biomedical applications. Biomed. Microdevices 2(1): 11-40.

Dubin, V.M., Vieillard, C., Ozanam, F. and Chazalviel, J.N. 1995. Preparation and characterization of surface-modified luminescent porous silicon. Phys. Status Solidi B 190(1): 47-52.

European Pharmacopoeia, 2009, 6th edition, Druckerei C.H. Beck, Nordlingen.

Fan, D.M., Akkaraju, G.R., Couch, E.F., Canham, L.T. and Coffer, J.L. 2011. The role of nanostructured mesoporous silicon in discriminating in vitro calcification for electrospun composite tissue engineering scaffolds. Nanoscale 3(2): 354-361.

Fathauer, R.W., George, T., Ksendzov, A. and Vasquez, R.P. 1992. Visible luminescence from silicon wafers subjected to stain etches. Appl. Phys. Lett. 60(8): 995-997.

Ferrari, M., Serda, R.E., Godin, B., Blanco, E. and Chiappini, C. 2011. Multi-stage delivery nano-particle systems for therapeutic applications. BBA - Gen. Subjects 1810(3): 317-329.

Foraker, A.B., Walczak, R.J., Cohen, M.H., Boiarski, T.A., Grove, C.F. and Swaan, P.W. 2003. Microfabricated porous silicon particles enhance paracellular delivery of insulin across intestinal Caco-2 cell monolayers. Pharm. Res. 20(1): 110-116.

GBI-Research. 2010. Money where the mouth is. World Pharma **2**, 77-80.

Godin, B., Gu, J., Serda, R.E., Bhavane, R., Tasciotti, E., Chiappini, C., Liu, X., Tanaka, T., Decuzzi, P. and Ferrari, M. 2010. Tailoring the degradation kinetics of mesoporous silicon structures through PEGylation. J. Biomed. Mater. Res. A 94A(4): 1236-1243.

Godin, B., Tasciotti, E., Liu, X., Serda, R.E. and Ferrari, M. 2011. Multistage nanovectors: from concept to novel imaging contrast agents and therapeutics. Acc. Chem. Res.

Goh, A.S.W., Chung, A.Y.F., Lo, R.H.G., Lau, T.N., Yu, S.W.K., Chng, M., Satchithanantham, S., Loong, S.L.E., Ng, D.C.E., Lim, B.C., Connor, S. and Chow, P.K.H. 2007. A novel approach to brachytherapy in hepatocellular carcinoma using a phosphorous(32) (P-32) brachytherapy delivery device - A first-in-man study. Int. J. Radiat. Oncol. 67(3): 786-792.

Gratton, S.E., Ropp, P.A., Pohlhaus, P.D., Luft, J.C., Madden, V.J., Napier, M.E. and DeSimone, J.M. 2008. The effect of particle design on cellular internalization pathways. Proc. Natl. Acad. Sci. U. S. A. 105(33): 11613-11618.

Grosman, A. and Ortega, C. (1997). Chemical composition of "fresh" porous silicon. Properties of Porous Silicon. Canham, L.T. London, Short Run Press Ltd.

Guerrero-Lemus, R., Ben-Hander, F., Hernández, R., amp, x, guez, C., Martı and nez-Duart, J.M. 2003. Optical and compositional characterisation of stain-etched porous silicon subjected to anodic oxidation and thermal treatments. Mater. Sci. Eng. B 101(1-3): 249-254.

Gupta, A.K. and Gupta, M. 2005. Cytotoxicity suppression and cellular uptake enhancement of surface modified magnetic nanoparticles. Biomaterials 26(13): 1565-1573.

Halimaoui, A. (1997). Porous silicon formation by anodisation. Properties of Porous Silicon. Canham, L. London, Short Run Press Ltd.

Hammer, M.U., Anderson, T.H., Chaimovich, A., Shell, M.S. and Israelachvili, J. 2010. The search for the hydrophobic force law. Faraday Discuss. 146: 299-308; discussion 367-293, 395-401.

Hauss, D.J. 2007. Oral lipid-based formulations. Adv. Drug Deliv. Rev. 59(7): 667-676.

He, Y., Fan, C. and Lee, S.-T. 2010. Silicon nanostructures for bioapplications. Nano Today 5(4): 282-295.

Hektor, H.J. and Scholtmeijer, K. 2005. Hydrophobins: proteins with potential. Curr. Opin. Biotech. 16(4): 434-439.

Hezi-Yamit, A., Sullivan, C., Wong, J., David, L., Chen, M., Cheng, P., Shumaker, D., Wilcox, J.N. and Udipi, K. 2009. Impact of polymer hydrophilicity on biocompatibility: Implication for DES polymer design. J. Biomed. Mater. Res. A 90A(1): 133-141.

Hoffman, A.S. 2008. The origins and evolution of "controlled" drug delivery systems. J. Control. Release 132(3): 153-163.

Huang, L.-F. and Tong, W.-Q. 2004. Impact of solid state properties on developability assessment of drug candidates. Adv. Drug Deliv. Rev. 56(3): 321-334

Jakubowicz, J., Smardz, K. and Smardz, L. 2007. Characterization of porous silicon prepared by powder technology. Physica E 38(1-2): 139-143.

Janssen, M.I., van Leeuwen, M.B., Scholtmeijer, K., van Kooten, T.G., Dijkhuizen, L. and Wosten, H.A. 2002. Coating with genetic engineered hydrophobin promotes growth of fibroblasts on a hydrophobic solid. Biomaterials 23(24): 4847-4854.

Jarvis, K.L., Barnes, T.J. and Prestidge, C.A. 2010. Thermal oxidation for controlling protein interactions with porous silicon. Langmuir 26(17): 14316-14322.

Jiang, W., Kim, B.Y., Rutka, J.T. and Chan, W.C. 2008. Nanoparticle-mediated cellular response is size-dependent. Nat. Nanotechnol. 3(3): 145-150.

Johansson, F., Wallman, L., Danielsen, N., Schouenborg, J. and Kanje, M. 2009. Porous silicon as a potential electrode material in a nerve repair setting: Tissue reactions. Acta Biomater. 5(6): 2230-2237.

Jugdaohsingh, R., Anderson, S.H., Tucker, K.L., Elliott, H., Kiel, D.P., Thompson, R.P. and Powell, J.J. 2002. Dietary silicon intake and absorption. Am. J. Clin. Nutr. 75(5): 887-893.

Jugdaohsingh, R., Tucker, K.L., Qiao, N., Cupples, L.A., Kiel, D.P. and Powell, J.J. 2004. Dietary silicon intake is positively associated with bone mineral density in men and premenopausal women of the Framingham Offspring cohort. J. Bone Miner. Res. 19(2): 297-307.

Karlsson, L.M., Schubert, M., Ashkenov, N. and Arwin, H. 2004. Protein adsorption in porous silicon gradients monitored by spatially-resolved spectroscopic ellipsometry. Thin Solid Films 455-456(0): 726-730.

Karlsson, L.M., Tengvall, P., Lundström, I. and Arwin, H. 2003. Penetration and loading of human serum albumin in porous silicon layers with different pore sizes and thicknesses. J. Colloid Interf. Sci. 266(1): 40-47.

Karp, J.M. and Langer, R. 2007. Development and therapeutic applications of advanced biomaterials. Curr. Opin. Biotechnol. 18(5): 454-459.

Kashanian, S., Harding, F., Irani, Y., Klebe, S., Marshall, K., Loni, A., Canham, L., Fan, D., Williams, K.A., Voelcker, N.H. and Coffer, J.L. 2010. Evaluation of mesoporous silicon/polycaprolactone composites as ophthalmic implants. Acta Biomater. 6(9): 3566-3572.

Kaukonen, A.M., Laitinen, L., Salonen, J., Tuura, J., Heikkila, T., Limnell, T., Hirvonen, J. and Lehto, V.P. 2007. Enhanced in vitro permeation of furosemide loaded into thermally carbonized mesoporous silicon (TCPSi) microparticles. Eur. J. Pharm. Biopharm. 66(3): 348-356.

Kawakami, K. 2009. Current status of amorphous formulation and other special dosage forms as formulations for early clinical phases. J. Pharm. Sci. 98(9): 2875-2885.

Kilpelainen, M., Monkare, J., Vlasova, M.A., Riikonen, J., Lehto, V.P., Salonen, J., Jarvinen, K. and Herzig, K.H. 2011. Nanostructured porous silicon microparticles enable sustained peptide (Melanotan II) delivery. Eur. J. Pharm. Biopharm. 77(1): 20-25.

Kilpelainen, M., Riikonen, J., Vlasova, M.A., Huotari, A., Lehto, V.P., Salonen, J., Herzig, K.H. and Jarvinen, K. 2009. In vivo delivery of a peptide, ghrelin antagonist, with mesoporous silicon microparticles. J. Control. Release 137(2): 166-170.

Kim, N.Y. and Laibinis, P.E. 1998. Derivatization of porous silicon by Grignard reagents at room temperature. J. Am. Chem. Soc. 120(18): 4516-4517.

Kocbach, A., Totlandsdal, A.I., Lag, M., Refsnes, M. and Schwarze, P.E. 2008. Differential binding of cytokines to environmentally relevant particles: a possible source for misinterpretation of in vitro results? Toxicol. Lett. 176(2): 131-137.

Kohane, D.S. and Langer, R. 2010. Biocompatibility and drug delivery systems. Chem. Sci. 1(4): 441-446.

Kolasinski, K.W. 2005. Silicon nanostructures from electroless electrochemical etching. Curr. Opin. Solid St. M. Science 9(1-2): 73-83.

Kolasinski, K.W., Hartline, J.D., Kelly, B.T. and Yadlovskiy, J. 2010. Dynamics of porous silicon formation by etching in HF + V2O5 solutions. Mol. Phys. 108(7-9): 1033-1043.

Kovalainen, M., Monkare, J., Makila, E., Salonen, J., Lehto, V.P., Herzig, K.H. and Jarvinen, K. 2011. Mesoporous silicon (PSi) for sustained peptide delivery: effect of PSi microparticle surface chemistry on peptide YY3-36 release. Pharm. Res. DOI: 10.1007/s11095-011-0611-6.

Kumar, R., Kitoh, Y. and Hara, K. 1993. Effect of surface treatment on visible luminescence of porous silicon: Correlation with hydrogen and oxygen terminators. Appl. Phys. Lett. 63(22): 3032-3034.

Kunzler, T.P., Drobek, T., Schuler, M. and Spencer, N.D. 2007. Systematic study of osteoblast and fibroblast response to roughness by means of surface-morphology gradients. Biomaterials 28(13): 2175-2182.

Kurppa, K., Jiang, H., Szilvay, G.R., Nasibulin, A.G., Kauppinen, E.L. and Linder, M.B. 2007. Controlled hybrid nanostructures through protein-mediated noncovalent functionalization of carbon nanotube. Angew. Chem. Int. Ed. 46(34): 6446-6449.

Laaksonen, P., Kainlauri, M., Laaksonen, T., Shchepetov, A., Jiang, H., Ahopelto, J. and Linder, M.B. 2010. Interfacial engineering by proteins: exfoliation and functionalization of graphene by hydrophobins. Angew. Chem. Int. Ed. 49(29): 4946-4949.

Laaksonen, T., Santos, H., Vihola, H., Salonen, J., Riikonen, J., Heikkila, T., Peltonen, L., Kumar, N., Murzin, D.Y., Lehto, V.P. and Hirvonen, J. 2007. Failure of MTT as a toxicity testing agent for mesoporous silicon microparticles. Chem. Res. Toxicol. 20(12): 1913-1918.

Lehmann, V. and Gösele, U. 1991. Porous silicon formation: A quantum wire effect. Appl. Phys Lett. 58(8): 856-858.

Lehmann, V., Stengl, R. and Luigart A. 2000. On the morphology and the electrochemical formation mechanism of mesoporous silicon. Mater. Sci. Eng. B 69-70(0): 11-22.

Lehto, V.P., Vähä-Heikkilä, K., Paski, J. and Salonen, J. 2005. Use of thermoanalytical methods in quantification of drug load in mesoporous silicon microparticles. J. Therm. Anal. Calorim. 80(2): 393-397.

Levy-Clement, C. 1995. Characteristic of porous n-type silicon obtained by photoelectrochemical etching. Porous Silicon Science and Technology. Vial, J.-C. and Derrien, J. Berlin, Springer-Verlag.

Li, K.H., Tsai, C., Campbell, J.C., Hance, B.K. and White, J.M. 1993. Investigation of rapid-thermal-oxidized porous silicon. Appl. Phys. Lett. 62(26): 3501-3503.

Limnell, T., Riikonen, J., Salonen, J., Kaukonen, A.M., Laitinen, L., Hirvonen, J. and Lehto, V.P. 2007. Surface chemistry and pore size affect carrier properties of mesoporous silicon microparticles. Int. J. Pharm. 343(1-2): 141-147.

Linder, M., Selber, K., Nakari-Setala, T., Qiao, M., Kula, M.R. and Penttila, M. 2001. The hydrophobins HFBI and HFBII from Trichoderma reesei showing efficient interactions with nonionic surfactants in aqueous two-phase systems. Biomacromolecules 2(2): 511-517.

Linder, M.B. 2009. Hydrophobins: Proteins that self assemble at interfaces. Curr. Opin. Colloid Interf. Sci. 14(5): 356-363.

Linford, M.R., Fenter, P., Eisenberger, P.M. and Chidsey, C.E.D. 1995. Alkyl monolayers on silicon prepared from 1-alkenes and hydrogen-terminated silicon. J. Am. Chem. Soc. 117(11): 3145-3155.

Lipinski, C.A. 2000. Drug-like properties and the causes of poor solubility and poor permeability. J. Pharmacol. Toxicol. 44(1): 235-249.

Lipinski, C.A., Lombardo, F., Dominy, B.W. and Feeney, P.J. 1997. Experimental and computational approaches to estimate solubility and permeability in drug discovery and development settings. Adv. Drug Deliv. Rev. 23(1-3): 3-25.

Liu, S., Palsule, C., Yi, S. and Gangopadhyay, S. 1994. Characterization of stain-etched porous silicon. Phys. Rev. B 49(15): 10318.

Loftsson, T. and Brewster, M.E. 2010. Pharmaceutical applications of cyclodextrins: basic science and product development. J. Pharm. Pharmacol. 62(11): 1607-1621.

Loftsson, T., Vogensen, S.B., Brewster, M.E. and Konradsdottir, F. 2007. Effects of cyclodextrins on drug delivery through biological membranes. J. Pharm. Sci. 96(10): 2532-2546.

Loni, A., Simons, A.J., Calcott, P.D.J., Newey, J.P., Cox, T.I. and Canham, L.T. 1997. Relationship between storage media and blue photoluminescence for oxidized porous silicon. Appl. Phys. Lett. 71(1): 107-109.

Lopez, C.A., Fleischman, A.J., Roy, S. and Desai, T.A. 2006. Evaluation of silicon nanoporous membranes and ECM-based microenvironments on neurosecretory cells. Biomaterials 27(16): 3075-3083.

Low, S.P., Williams, K.A., Canham, L.T. and Voelcker, N.H. 2006. Evaluation of mammalian cell adhesion on surface-modified porous silicon. Biomaterials 27(26): 4538-4546.

Low, S.P., Williams, K.A., Canham, L.T. and Voelcker, N.H. 2010. Generation of reactive oxygen species from porous silicon microparticles in cell culture medium. J. Biomed. Mater. Res. A 93(3): 1124-1131.

Low, S.P., Voelcker, N.H., Canham, L.T. and Williams, K.A. 2009. The biocompatibility of porous silicon in tissues of the eye. Biomaterials 30(15): 2873-2880.

Lumsdon, S.O., Green, J. and Stieglitz, B. 2005. Adsorption of hydrophobin proteins at hydrophobic and hydrophilic interfaces. Colloids Surf. B 44(4): 172-178.

Martinez, M.N. and Amidon, G.L. 2002. A mechanistic approach to understanding the factors affecting drug absorption: A review of fundamentals. J. Clin. Pharmacol. 42(6): 620-643.

Mawhinney, D.B., Glass, J.A. and Yates, J.T. 1997. FTIR study of the oxidation of porous silicon. J. Phys. Chem. B 101(7): 1202-1206.

McNaught, A.D. and Wilkinson, A. 1997. IUPAC. Compendium of Chemical Terminology. Oxford, Blackwell Scientific Publications.

Meyer, E.E., Rosenberg, K.J. and Israelachvili, J. 2006. Recent progress in understanding hydrophobic interactions. Proc. Natl. Acad. Sci. U. S. A. 103(43): 15739-15746.

Mitragotri, S. and Lahann, J. 2009. Physical approaches to biomaterial design. Nat. Mater. 8(1): 15-23.

Moghimi, S.M., Hunter, A.C. and Murray, J.C. 2005. Nanomedicine: current status and future prospects. FASEB J. 19(3): 311-330.

Monteiro-Riviere, N.A., Inman, A.O. and Zhang, L.W. 2009. Limitations and relative utility of screening assays to assess engineered nanoparticle toxicity in a human cell line. Toxicol. Appl. Pharmacol. 234(2): 222-235.

Müller, J.M., Rupec, R.A. and Baeuerle, P.A. 1997. Study of gene regulation by NF-κB and AP-1 in response to reactive oxygen intermediates. Methods 11(3): 301-312.

Myllymaa, S., Myllymaa, K., Korhonen, H., Lammi, M.J., Tiitu, V. and Lappalainen, R. 2010. Surface characterization and in vitro biocompatibility assessment of photosensitive polyimide films. Colloids Surf. B 76(2): 505-511.

Nel, A., Xia, T., Madler, L. and Li, N. 2006. Toxic potential of materials at the nanolevel. Science 311(5761): 622-627.

Nijdam, A.J., Ming-Cheng Cheng, M., Geho, D.H., Fedele, R., Herrmann, P., Killian, K., Espina, V., Petricoin Iii, E.F., Liotta, L.A. and Ferrari, M. 2007. Physicochemically modified silicon as a substrate for protein microarrays. Biomaterials 28(3): 550-558.

Nijdam, A.J., Zianni, M.R., Herderick, E.E., Cheng, M.M.C., Prosperi, J.R., Robertson, F.A., Petricoin, E.F., Liotta, L.A. and Ferrari, M. 2009. Application of physicochemically modified silicon substrates as reverse-phase protein microarrays. J. Proteome Res. 8(3): 1247-1254.

Noguchi, N. and Suemune, I. 1993. Luminescent porous silicon synthesized by visible light irradiation. Appl. Phys. Lett. 62(12): 1429-1431.

O'Lenick, A.J. 2009. Basic silicone chemistry - a review. Silicone Spectator 1-23

Oberdorster, G. 2010. Safety assessment for nanotechnology and nanomedicine: concepts of nanotoxicology. J. Intern. Med. 267(1): 89-105.

Palestino, G., Agarwal, V., Aulombard, R., Pérez, E.a. and Gergely, C. 2008. Biosensing and protein fluorescence enhancement by functionalized porous silicon devices. Langmuir 24(23): 13765-13771.

Parbukov, A.N., Beklemyshev, V.I., Gontar, V.M., Makhonin, I.I., Gavrilov, S.A. and Bayliss, S.C. 2001. The production of a novel stain-etched porous silicon, metallization of the porous surface and application in hydrocarbon sensors. Mater. Sci. Eng. C 15(1-2): 121-123.

Park, J.H., Gu, L., von Maltzahn, G., Ruoslahti, E., Bhatia, S.N. and Sailor, M.J. 2009. Biodegradable luminescent porous silicon nanoparticles for in vivo applications. Nat. Mater .8(4): 331-336.

Peer, D., Karp, J.M., Hong, S., Farokhzad, O.C., Margalit, R. and Langer, R. 2007. Nanocarriers as an emerging platform for cancer therapy. Nat. Nanotechnol. 2(12): 751-760.

Perelman, L.A., Pacholski, C., Li, Y.Y., VanNieuwenhz, M.S. and Sailor, M.J. 2008. pH-triggered release of vancomycin protein-capped porous silicon films from. Nanomedicine-UK 3(1): 31-43.

Petrova-Koch, V., Muschik, T., Kux, A., Meyer, B.K., Koch, F. and Lehmann, V. 1992. Rapid-thermal-oxidized porous Si-The superior photoluminescent Si. Appl. Phys. Lett. 61(8): 943-945.

Popplewell, J.F., King, S.J., Day, J.P., Ackrill, P., Fifield, L.K., Cresswell, R.G., di Tada, M.L. and Liu, K. 1998. Kinetics of uptake and elimination of silicic acid by a human subject: a novel application of 32Si and accelerator mass spectrometry. J. Inorg. Biochem. 69(3): 177-180.

Poznansky, M.J. and Juliano, R.L. 1984. Biological approaches to the controlled delivery of drugs - a critical-review. Pharmacol. Rev. 36(4): 277-336.

Prestidge, C.A., Barnes, T.J., Lau, C.-H., Barnett, C., Loni, A. and Canham, L. 2007. Mesoporous silicon: a platform for the delivery of therapeutics. Expert Opin. Drug Deliv. 4(2): 101-110.

Prestidge, C.A., Barnes, T.J., Mierczynska-Vasilev, A., Skinner, W., Peddie, F. and Barnett, C. 2007. Loading and release of a model protein from porous silicon powders. Phys. Status Solidi A 204(10): 3361-3366.

Prestidge, C.A., Barnes, T.J., Mierczynska-Vasilevl, A., Kempson, I., Peddiel, F. and Barnett, C. 2008. Peptide and protein loading into porous silicon wafers. Phys. Status Solidi A 205(2): 311-315.

Richmond, P. 1974. Electrical forces between particles with arbitrary fixed surface charge distributions in ionic solution. J. Chem. Soc. 70: 1066-1073.

Riikonen, J., Makila, E., Salonen, J. and Lehto, V.P. 2009. Determination of the physical state of drug molecules in mesoporous silicon with different surface chemistries. Langmuir 25(11): 6137-6142.

Rosengren, A., Wallman, L., Bengtsson, M., Laurell, T., Danielsen, N. and Bjursten, L.M. 2000. Tissue reactions to porous silicon: a comparative biomaterial study. Phys. Status Solidi A 182(1): 527-531.

Rouquerol, J., Avnir, D., Fairbridge, C.W., Everett, D.H., Haynes, J.H., Pernicone, N., Ramsay, J.D.F., Sing, K.S.W. and Unger, K.K. 1994. Recommendations for the characterization of porous solids. Pure Appl. Chem. 66(8): 1739-1758.

Sailor, M.J. and Song, J.H. 1998. Functionalization of nanocrystalline porous silicon surfaces with aryllithium reagents: Formation of silicon-carbon bonds by cleavage of silicon-silicon bonds. J. Am. Chem. Soc. 120(10): 2376-2381.

Salonen, J., Bjorkqvist, M., Laine, E. and Niinisto, L. 2004. Stabilization of porous silicon surface by thermal decomposition of acetylene. Appl. Surf. Sci. 225(1-4): 389-394.

Salonen, J., Björkqvist, M., Laine, E. and Niinistö, L. 2000. Effects of fabrication parameters on porous p+-type silicon morphology. Phys. Status Solidi A 182(1): 249-254.

Salonen, J., Kaukonen, A.M., Hirvonen, J. and Lehto, V.P. 2008. Mesoporous silicon in drug delivery applications. J. Pharm. Sci. 97(2): 632-653.

Salonen, J., Laitinen, L., Kaukonen, A.M., Tuura, J., Bjorkqvist, M., Heikkila, T., Vaha-Heikkila, K., Hirvonen, J. and Lehto, V.P. 2005. Mesoporous silicon microparticles for oral drug delivery: loading and release of five model drugs. J. Control. Release 108(2-3): 362-374.

Salonen, J. and Lehto, V.-P. 2008. Fabrication and chemical surface modification of mesoporous silicon for biomedical applications. Chem. Eng. J. 137(1): 162-172.

Salonen, J., Lehto, V.-P. and Laine, E. 1997. Thermal oxidation of free-standing porous silicon films Appl. Phys. Lett. 70(5): 637-639.

Santini, J.T., Cima, M.J. and Langer, R. 1999. A controlled-release microchip. Nature 397(6717): 335-338.

Santos, H.A., Bimbo, L.M., Lehto, V.P., Airaksinen, A.J., Salonen, J. and Hirvonen, J. 2011. Multifunctional porous silicon for therapeutic drug delivery and imaging. Curr. Drug Discov. Technol. 8(3): 228-249.

Santos, H.A., Riikonen, J., Salonen, J., Makila, E., Heikkila, T., Laaksonen, T., Peltonen, L., Lehto, V.P. and Hirvonen, J. 2010. In vitro cytotoxicity of porous silicon

microparticles: Effect of the particle concentration, surface chemistry and size. Acta Biomater. 6(7): 2721-2731.

Sapelkin, A.V., Bayliss, S.C., Unal, B. and Charalambou, A. 2006. Interaction of B50 rat hippocampal cells with stain-etched porous silicon. Biomaterials 27(6): 842-846.

Sarparanta, M., Bimbo, L.M., Mäkilä, E., Laaksonen, T., Laaksonen, P., Nyman, P., Salonen, J., Linder, M.B., Hirvonen, J., Santos, H.A. and Airaksinen, A.J. 2011. Hydrophobin-coated thermally hydrocarbonized porous silicon nanoparticles: stability protein adsorption and biodistribution. (Submitted).

Scheel, J., Weimans, S., Thiemann, A., Heisler, E. and Hermann, M. 2009. Exposure of the murine RAW 264.7 macrophage cell line to hydroxyapatite dispersions of various composition and morphology: assessment of cytotoxicity, activation and stress response. Toxicol. In Vitro 23(3): 531-538.

Schou, M., Halldin, C., Sovago, J., Pike, V.W., Hall, H., Gulyas, B., Mozley, P.D., Dobson, D., Shchukin, E., Innis, R.B. and Farde, L. 2004. PET evaluation of novel radiofluorinated reboxetine analogs as norepinephrine transporter probes in the monkey brain. Synapse 53(2): 57-67.

Sciacca, B., Alvarez, S.D., Geobaldo, F. and Sailor, M.J. 2010. Bioconjugate functionalization of thermally carbonized porous silicon using a radical coupling reaction. Dalton T. 39(45): 10847-10853.

Serda, R.E., Ferrati, S., Godin, B., Tasciotti, E., Liu, X. and Ferrari, M. 2009. Mitotic trafficking of silicon microparticles. Nanoscale 1(2): 250-259.

Serda, R.E., Go, J.H., Bhavane, R.C., Liu, X.W., Chiappini, C., Decuzzi, P. and Ferrari, M. 2009. The association of silicon microparticles with endothelial cells in drug delivery to the vasculature. Biomaterials 30(13): 2440-2448.

Serda, R.E., Gu, J., Burks, J.K., Ferrari, K., Ferrari, C. and Ferrari, M. 2009. Quantitative mechanics of endothelial phagocytosis of silicon microparticles. Cytom. Part A 75A(9): 752-760.

Serda, R.E., Mack, A., Pulikkathara, M., Zaske, A.M., Chiappini, C., Fakhoury, J., Webb, D., Godin, B., Conyers, J.L., Liu, X.W., Bankson, J.A. and Ferrari, M. 2010. Cellular association and assembly of a multistage delivery system. Small.

Serda, R.E., Blanco, E., Mack, A., Stafford, S.J., Amra, S., Li, Q., van de Ven, A., Tanaka, T., Torchilin, V.P., Wiktorowicz, J.E. and Ferrari, M. 2011. Proteomic analysis of serum opsonins impacting biodistribution and cellular association of porous silicon microparticles. Mol. Imaging 10(1): 43-55.

Serda, R.E., Godin, B., Blanco, E., Chiappini, C. and Ferrari, M. 2011. Multi-stage delivery nano-particle systems for therapeutic applications. BBA - Gen. Subjects 1810(3): 317-329.

Seregin, V.V. and Coffer, J.L. 2006. Bias-assisted in vitro calcification of calcium disilicide growth layers on spark-processed silicon. Biomaterials 27(20): 3726-3737.

Sharma, S., Nijdam, A.J., Sinha, P.M., Walczak, R.J., Liu, X., Cheng, M.M.-C. and Ferrari, M. 2006. Controlled-release microchips. Expert Opin. Drug Deliv. 3(3): 379-394.

Shih, S., Jung, K.H., Hsieh, T.Y., Sarathy, J., Campbell, J.C. and Kwong, D.L. 1992. Photoluminescence and formation mechanism of chemically etched silicon. Appl. Phys. Lett. 60(15): 1863-1865.

Singh, A., Worku, Z.A. and Van den Mooter, G. 2011. Oral formulation strategies to improve solubility of poorly water-soluble drugs. Expert. Opin. Drug. Deliv. 8(10): 1361-1378

Smith, R.L. and Collins, S.D. 1992. Porous silicon formation mechanisms. J. Appl. Phys. 71(8): R1-R22.

Smolen, V.F. 1978. Bioavailability and pharmacokinetic analysis of drug responding systems. Annu. Rev. Pharmacol. Toxicol. 18: 495-522.

Soref, R.A. 1993. Silicon-based optoelectronics. Proceedings of the IEEE 81(12): 1687-1706.

Stewart, M.P. and Buriak, J.M. 2000. Chemical and biological applications of porous silicon technology. Adv. Mater. 12(12): 859-869.

Takazawa, A., Tamura, T. and Yamada, M. 1994. Photoluminescence mechanisms of porous Si oxidized by dry oxygen. J. Appl. Phys. 75(5): 2489-2495.

Tanaka, T., Godin, B., Bhavane, R., Nieves-Alicea, R., Gu, J., Liu, X., Chiappini, C., Fakhoury, J.R., Amra, S., Ewing, A., Li, Q., Fidler, I.J. and Ferrari, M. 2010. In vivo evaluation of safety of nanoporous silicon carriers following single and multiple dose intravenous administrations in mice. Int. J. Pharm. 402(1-2): 190-197.

Tanaka, T., Mangala, L.S., Vivas-Mejia, P.E., Nieves-Alicea, R., Mann, A.P., Mora, E., Han, H.D., Shahzad, M.M., Liu, X., Bhavane, R., Gu, J., Fakhoury, J.R., Chiappini, C., Lu, C., Matsuo, K., Godin, B., Stone, R.L., Nick, A.M., Lopez-Berestein, G., Sood, A.K. and Ferrari, M. 2010. Sustained small interfering RNA delivery by mesoporous silicon particles. Cancer Res. 70(9): 3687-3696.

Tasciotti, E., Liu, X., Bhavane, R., Plant, K., Leonard, A.D., Price, B.K., Cheng, M.M., Decuzzi, P., Tour, J.M., Robertson, F. and Ferrari, M. 2008. Mesoporous silicon particles as a multistage delivery system for imaging and therapeutic applications. Nat. Nanotechnol. 3(3): 151-157.

Tasciotti, E., Godin, B., Martinez, J.O., Chiappini, C., Bhavane, R., Liu, X.W. and Ferrari, M. 2011. Near-infrared imaging method for the in vivo assessment of the biodistribution of nanoporous silicon particles. Mol. Imaging 10(1): 56-68.

Tavares, J.C., Cornelio, D.A., da Silva, N.B., de Moura, C.E., de Queiroz, J.D., Sa, J.C., Alves, C., Jr. and de Medeiros, S.R. 2009. Effect of titanium surface modified by plasma energy source on genotoxic response in vitro. Toxicology 262(2): 138-145.

Trachootham, D., Lu, W., Ogasawara, M.A., Valle, N.R.-D. and Huang, P. 2008. Redox regulation of cell survival. Antiox. Redox Sign. 10(8): 1343-1374.

Uhlir, A. 1956. Electrolytic shaping of germanium and silicon. Bell System Tech. J. 35: 333-347.

USP 2003/2009, 26th /32nd edition, United States Pharmacopoeial Convention, Rockville MD.

Vaccari, L., Canton, D., Zaffaroni, N., Villa, R., Tormen, M. and di Fabrizio, E. 2006. Porous silicon as drug carrier for controlled delivery of doxorubicin anticancer agent. Microelectron. Eng. 83(4-9): 1598-1601.

Vallet-Regí, M., Balas, F. and Arcos, D. 2007. Mesoporous materials for drug delivery. Angew. Chem. Int. Ed. 46(40): 7548-7558.

Valo, H.K., Laaksonen, P.H., Peltonen, L.J., Linder, M.B., Hirvonen, J.T. and Laaksonen, T.J. 2010. Multifunctional hydrophobin: toward functional coatings for drug nanoparticles. ACS Nano 4(3): 1750-1758.

Valo, H.K, Kovalainen, M., Laaksonen, P., Hakkinen, M., Auriola, S., Peltonen, L., Linder, M., Jarvinen, K., Hirvonen, J. and Laaksonen, T. 2011. Immobilization of protein-coated drug nanoparticles in nanofibrillar cellulose matrices: enhanced stability and release. J. Control. Release. DOI:10.1016/j.jconrel.2011.07.016.

van Breemen, R.B. and Li, Y. 2005. Caco-2 cell permeability assays to measure drug absorption. Expert Opin. Drug Metab. Toxicol. 1(2): 175-185.

Varjonen, S., Laaksonen, P., Paananen, A., Valo, H., Hahl, H., Laaksonen, T. and Ben Linder, M. 2011. Self-assembly of cellulose nanofibrils by genetically engineered fusion proteins. Soft Matter 7(6): 2402-2411.

Walczyk, D., Bombelli, F.B., Monopoli, M.P., Lynch, I. and Dawson, K.A. 2010. What the cell "sees" in bionanoscience. J. Am. Chem. Soc. 132(16): 5761-5768.

Wang, F., Hui, H., Barnes, T.J., Barnett, C. and Prestidge, C.A. 2010. Oxidized mesoporous silicon microparticles for improved oral delivery of poorly soluble drugs. Mol. Pharm. 7(1): 227-236.

Wang, M., Coffer, J.L., Dorraj, K., Hartman, P.S., Loni, A. and Canham, L.T. 2010. Sustained antibacterial activity from triclosan-loaded nanostructured mesoporous silicon. Mol. Pharm. 7(6): 2232-2239.

Wang, Z., Lienemann, M., Qiau, M. and Linder, M.B. 2010. Mechanisms of protein adhesion on surface films of hydrophobin. Langmuir 26(11): 8491-8496.

Watanabe, Y. and Sakai, T. 1971. Application of a thick anode film to semiconductor devices. Rev. Elec. Commun. Lab. 19(7-8): 899-&.

West, J.L. and Halas, N.J. 2003. Engineered nanomaterials for biophotonics applications: improving sensing, imaging, and therapeutics. Annu. Rev. Biomed. Eng. 5(1): 285-292.

Won, C.W., Nersisyan, H.H., Shin, C.Y. and Lee, J.H. 2009. Porous silicon microparticles synthesis by solid flame technique. Micropor. Mesopor. Mat. 126(1-2): 166-170.

Wu, E.C., Park, J.-H., Park, J., Segal, E., Cunin, F. and Sailor, M.J. 2008. Oxidation-triggered release of fluorescent molecules or drugs from mesoporous Si microparticles. ACS Nano 2(11): 2401-2409.

Wu, E.C., Andrew, J.S., Buyanin, A., Kinsella, J.M. and Sailor, M.J. 2011. Suitability of porous silicon microparticles for the long-term delivery of redox-active therapeutics. Chem. Commun. (Camb) 47(20): 5699-5701.

Wu, E.C., Andrew, J.S., Cheng, L., Freeman, W.R., Pearson, L. and Sailor, M.J. 2011. Real-time monitoring of sustained drug release using the optical properties of porous silicon photonic crystal particles. Biomaterials 32(7): 1957-1966.

Xiao, L., Gu, L., Howell, S.B. and Sailor, M.J. 2011. Porous silicon nanoparticle photosensitizers for singlet oxygen and their phototoxicity against cancer cells. ACS Nano 5(5): 3651-3659.

Xue, M., Zhong, X., Shaposhnik, Z., Qu, Y., Tamanoi, F., Duan, X. and Zink, J.I. 2011. pH-Operated mechanized porous silicon nanoparticles. J. Am. Chem. Soc. 133(23): 8798-8801.

Yaroshevsky, A. 2006. Abundances of chemical elements in the Earth's crust. Geochem. Int. 44(1): 48-55.

Yee, S. 1997. In vitro permeability across Caco-2 cells (colonic) can predict in vivo (small intestinal) absorption in man--fact or myth. Pharm. Res. 14(6): 763-766.

Yoo, J.-W., Doshi, N. and Mitragotri, S. 2010. Endocytosis and intracellular distribution of PLGA particles in endothelial cells: effect of particle geometry. Macromol. Rapid Commun. 31(2): 142-148.

Yoo, J.-W., Irvine, D.J., Discher, D.E. and Mitragotri, S. 2011. Bio-inspired, bioengineered and biomimetic drug delivery carriers. Nat. Rev. Drug Discov. 10(7): 521-535.

Yu, L. 2001. Amorphous pharmaceutical solids: preparation, characterization and stabilization. Adv. Drug Deliv. Rev. 48(1): 27-42.

Zangooie, S., Bjorklund, R. and Arwin, H. 1998. Protein adsorption in thermally oxidized porous silicon layers. Thin Solid Films 313: 825-830.

Zazzera, L.A., Evans, J.F., Deruelle, M., Tirrell, M., Kessel, C.R. and Mckeown, P. 1997. Bonding organic molecules to hydrogen-terminated silicon wafers. J. Electrochem. Soc. 144(6): 2184-2189.

Zhang, G. (2001). Electrochemistry of silicon and its oxides. Secaucus, NJ, USA, Kluwer Academic Publishers.

Zhang, K., Loong, S.L.E., Connor, S., Yu, S.W.K., Tan, S.Y., Ng, R.T.H., Lee, K.M., Canham, L. and Chow, P.K.H. 2005. Complete tumor response following intratumoral P-32 BioSilicon on human hepatocellular and pancreatic carcinoma xenografts in nude mice. Clin. Cancer Res. 11(20): 7532-7537.